NASA Technical Paper 1501

Evaluation of a Wind-Tunnel Gust Response Technique Including Correlations With Analytical and Flight Test Results

L. Tracy Redd, Perry W. Hanson,
and Eleanor C. Wynne

NOVEMBER 1979

NASA

NASA Technical Paper 1501

Evaluation of a Wind-Tunnel Gust Response Technique Including Correlations With Analytical and Flight Test Results

L. Tracy Redd, Perry W. Hanson,
and Eleanor C. Wynne
Langley Research Center
Hampton, Virginia

National Aeronautics
and Space Administration

**Scientific and Technical
Information Branch**

1979

SUMMARY

A wind-tunnel technique for obtaining gust frequency-response functions for use in predicting the response of flexible aircraft to atmospheric turbulence is evaluated by comparing the tunnel test results for a dynamically scaled cable-supported aeroelastic model with analytical and flight data. The technique, which employs oscillating vanes in the tunnel throat section to generate a sinusoidally varying flow field around the model, was evaluated by use of a 1/30-scale model of the B-52E airplane, for which considerable flight gust response data were available. The studies show good correlation between the wind-tunnel results, flight test results, and analytical predictions for response in the short-period and wing first elastic modes of motion, which are the modes of primary significance for response of flexible aircraft to atmospheric turbulence.

INTRODUCTION

The response of aircraft to atmospheric turbulence is an important design consideration from the standpoint of gust loads, structural fatigue, and ride quality. A method commonly used to determine the response of aircraft to random gusts is based on random process theory or the so-called power spectral analysis technique (see refs. 1 and 2, for example). In this method the response of a flexible airplane is determined for excitation by sinusoidal gusts of varying frequency. This response function is commonly referred to as the frequency-response function.

Airplane frequency-response functions are generally determined from power spectral data measured during flight tests (ref. 3) or by analytical methods (refs. 4 to 7). The procedures for determining response functions from flight tests are costly; furthermore, they cannot provide early design data for specific configurations. Analytical methods, on the other hand, may prove to be inadequate, particularly in the transonic speed range, where accurate definition of unsteady aerodynamic loads is lacking. Therefore, a wind-tunnel method is desirable for evaluating frequency-response functions experimentally under controlled conditions during the design phase. Such a method would allow verification of the analysis in a timely manner. The need for a controlled experimental method led to the development of a unique wind-tunnel gust response technique developed for use in the Langley transonic dynamics tunnel.

The wind-tunnel technique consists of measuring the response of an aeroelastically scaled model to an oscillating vertical gust field generated in the tunnel by oscillating vanes located upstream of the test section. The model is flown on a two-cable support system (ref. 8) which permits simulation of free-flight modes of motion. Two preliminary model studies (refs. 9 and 10) using the technique showed good correlation between analysis and wind-tunnel response measurements for rigid body modes of motion.

The next logical step in the verification of the method was to conduct tests using a dynamically scaled aeroelastic model and to compare the results with analytical predictions and flight data. Because considerable gust response data were available for the B-52E airplane, it was selected as the test vehicle for a comparative analysis of the wind-tunnel, flight, and analytical test methods. The study was conducted through an effort carried out jointly by NASA, the U.S. Air Force, and the Boeing Company (Wichita Division). This paper describes the B-52E model wind-tunnel tests involved in the study and compares those test results with analytical and flight data.

SYMBOLS AND ABBREVIATIONS

C_b wing vertical bending-moment coefficient, $M_b/qS\bar{c}$

C_n coefficent of normal acceleration, $m\ddot{z}/qS$

C_q dynamic pitching-moment coefficient, $\partial\bar{c}w/2Vq$S

$\bar{c}$ mean aerodynamic chord, m

c.g. center of gravity

d_v distance from oscillating vane quarter chord to gust probe head (14.9 m)

F.S. model body station measured along fuselage center line (F.S. 0 is 4.83 cm forward of fuselage nose), m

f frequency, Hz

g gravitational constant, 9.80 m/sec^2

k reduced frequency, $\bar{c}\omega/2V$

L.W.S. left wing station

l characteristic length, m

M Mach number

M_b wing vertical bending moment, N-m

m mass, kg

P.R.G. pitch-rate gyro

q dynamic pressure, Pa

R.W.S. right wing station

S wing area, m^2

V velocity, m/sec

W weight, N

W.S. wing station, measured parallel to wing trailing edge (W.S. 0 is at intersection of wing leading edge and fuselage center line), cm

$\ddot{z}$ vertical acceleration normal to fuselage center line, m/sec^2

$|\epsilon_g|$ absolute value of measured gust amplitude, deg

$|\bar{\epsilon}_g|$ absolute averaged value of gust amplitude over wing span, deg

δ_v oscillating amplitude of gust vanes, deg

ρ atmospheric air or tunnel test-medium density, kg/m^3

ϕ phase angle between model response and gust, deg

ϕ_d theoretical phase angle between gust at model c.g. and gust vane, deg

ϕ_g measured phase angle between gust at model c.g. and gust vane, deg

$\bar{\phi}_g$ averaged value of gust phase angle along model wing span, deg

ω circular frequency, $2\pi f$, rad/sec

Subscripts:

A full-scale airplane

M model

APPARATUS

The study was conducted in the Langley transonic dynamics tunnel which has a 4.88-m slotted test section and is capable of testing at Mach numbers up to 1.2 in air or Freon-12, over a wide range of air or test-medium densities. The tunnel is capable of generating a simulated (sinusoidal) gust field in the test section.

The main features of the oscillating vane system used to generate the gust field are shown in figure 1. Two sets of vanes, in a biplane arrangement, are located on the side walls of the entrance section of the tunnel. The vanes have a span of 1.07 m, a taper ratio of 0.5, and a panel aspect ratio of 1.2. The biplane vanes on each wall are oscillated about the quarter chord by a hydraulic motor and a large flywheel by means of linkages, which produce nearly sinusoidal vane oscillations about the mean angle-of-attack position. Under normal circumstances, the vane amplitudes are mechanically adjustable from 0° to $\pm 12^\circ$, and

the frequency is remotely adjustable from 0 to 20 Hz by means of an electrical control system which also synchronizes the motions of the two sets of vanes. By means of this system, the phasing of the two sides can be varied from "in sync" to 180° out of synchronization; however, this capability was not used in this investigation.

The flow angle of the airstream was measured with four differential pressure probes mounted 0.61 m apart on a horizontal bar as shown in figure 2. The bar was attached to a stand which could be located at any longitudinal station in the tunnel. The bar could be adjusted to any vertical station within a distance of ±0.61 m from the center of the test section and could be remotely traversed laterally on the support, ±0.30 m from the tunnel center line.

The pressure probes (fig. 3) consisted of two (0.178 cm inner diameter) steel tubes or "claws," attached to opposite sides of a two-arm variable-reluctance differential pressure transducer. The claws of the probes were oriented to measure flow angularity in the vertical plane by means of the attendant pressure differential between the upper and lower claw tubes.

Flow angle measurements in the test section were made in the vicinity of the model center of gravity (c.g.), which was located approximately 14.9 m downstream of the vane quarter chord.

FLOW FIELD

Measurements of the flow field generated by the airstream oscillator are shown in figures 4 and 5. Figure 4 presents a three-dimensional view of the variation of gust amplitude $|\epsilon_g|$ and phase angle ϕ_g as a function of lateral position in the tunnel and vane oscillation reduced frequency. These plots were made by fitting a surface spline (ref. 11) through the measured data points (shown as circles in the figure). These figures indicate that the amplitude decreases and the phase lag decreases linearly with increasing frequency. All the data shown are based on 1-minute averages of the output of an electronic sine-cosine resolver system that gives the in-phase and out-of-phase components of the first harmonic of stream angle with respect to vane position. This procedure was used to average out the effect of random tunnel turbulence.

The data shown in the figures are for a velocity of 35.4 m/sec, which is required to simulate the velocity of the full-scale airplane. The vane amplitude (±6°) was determined from the practical consideration that the gust angle at the model c.g. must be large enough to excite the short-period and lower elastic modes, but not so large that the model could be damaged. These data show a considerable variation in gust amplitude in the spanwise direction at low frequencies. The phase data are fairly uniform in the spanwise direction, except at the higher frequencies. Although there is considerable variation in spanwise gust amplitude at low frequencies, the gust is sufficiently uniform to produce model responses similar to those predicted for a gust uniformly distributed over the wing span. This fact is shown in the data presented in following sections. Consequently, the spanwise variations in the gust amplitude and phase angle were averaged across the span for each value of reduced frequency k in

analyzing the model gust response data. The results of this averaging process are shown in figures 5(a) and 5(b). The format used in figure 5(b) confines variations of the phase angle data to $\pm 180^{\circ}$ (instead of accumulating to -1400° as in fig. 4(b)). At low reduced frequencies the measured phase angle ϕ_g approximates that predicted by the equation

$$\phi_d = -360 \frac{fd_v}{V}$$

where ϕ_d is the phase difference caused by the time required for a point on a traveling wave at a frequency f to move downstream the distance from the vane quarter chord to the probe head d_v at a velocity V. The difference between the measured and the theoretical phase lag at high reduced frequencies can be attributed to unsteady flow effects on the vanes.

MODEL PROPERTIES AND INSTRUMENTATION

Model Scaling Considerations

The 1/30-geometric-scale model was designed to simulate the B-52E airplane dynamically and aeroelastically at a gross mass of 189 964 kg at a flight altitude of 1646 m with external tanks attached. Froude number, reduced frequency, and mass ratio of the model and airplane were matched. The model stiffness properties, inertia properties (distributed masses and moments of inertia), aerodynamic properties, and center-of-gravity location also matched that of the full-scale B-52E airplane. The model scaling factors derived from the preceding conditions are tabulated in table I.

To simulate the airplane altitude (air density) and to allow the model to be heavy enough for instrumentation and ballasting, the tests were carried out in Freon-12 gas. The resulting density ratio of 4.07 between model and airplane (see table I) provided a model mass of 28.7 kg. Comparisons of the model airplane test conditions and other parameters are given in table II.

Model Physical Characteristics

The model is shown mounted in the Langley transonic dynamics tunnel in figure 6, and a schematic diagram of the mount system is shown in figure 7. The system (ref. 8) consists of two "flying" cables on which the model is suspended. The forward flying cable loop is in the vertical plane; the rear flying cable loop is in the horizontal plane. Four "snubber cables," normally slack during testing, can be remotely activated to snub or restrain the model in case an instability occurs.

To achieve reasonable simulation of the short-period mode of the B-52E airplane, the basic two-cable-mount system of reference 8 was modified as shown in

figure 7. In this case, the cables were attached through pivots to the model near the center of gravity, and the pulleys were mounted at the tunnel wall instead of following the normal positioning of the pulleys inside the contour of the model fuselage. This modification resulted in a mount configuration which had a rotational stiffness low enough in pitch to allow adequate simulation of the short-period free-flight mode.

Except for the vertical tail, the model stiffness was provided by aluminum alloy spars covered with separate rigid fairing sections which provided the aerodynamic contour of the airplane. Each section was attached to the spars independently so that stiffness of the spars would not be altered. Nacelle stiffness was provided by a single mounting strut attached to the wing spar. The vertical tail had an aluminum plate core with balsa covering to provide the airfoil shape.

The model geometry is shown in figure 8. The ailerons and all-movable horizontal stabilizers provided roll and pitch trim control, respectively, and both controls could be operated remotely from the tunnel control room.

Model Dynamic Characteristics

Before the wind-tunnel testing was begun, the model was mounted on the flying cables in the tunnel test section, and model ground vibration tests were conducted in the wind-off condition. The suspension system used allowed proper simulation of the airplane short-period mode. A soft spring attached to the model at the c.g. was used to suspend the model vertically in the tunnel for these vibration tests. A comparison of the symmetric modal frequencies measured in these tests and those calculated for the unrestrained model are shown in tables III and IV. The data show that calculated and measured frequencies of the flexible modes (table III(a)) are in good agreement. The agreement between calculated and measured rigid body modes (table III(b)) and nacelle strut modes (table IV) is considered adequate.

The modal node lines obtained in the model vibration tests are shown in figure 9 for the first four symmetric elastic modes. These are the modes which were most readily excited by the gust velocity generated in the tunnel. As shown in figure 4, the gust amplitude is almost zero above a reduced frequency of 0.20 (which corresponds to a frequency of about 10 Hz).

Instrumentation

Locations of the onboard instrumentation and equipment for measuring the model response and for powering the horizontal stabilizer and aileron control surfaces are shown in figure 10. The sensors consisted of (1) four sets of strain-gage bridges mounted on the wing spar, oriented and calibrated to measure bending moments; (2) three vertical accelerometers mounted on the fuselage spar; and (3) a pitch-rate gyro mounted on the fuselage spar at the model c.g. Aileron and stabilizer control surfaces were driven by independent dc torque motors

through crank-pushrod linkages. The pushrods were connected by flexible bellows couplings. The aileron motors each provided a maximum torque of ±0.381 N-m, and through the linkages, control surface oscillation amplitude of ±25° was provided in the frequency range from 0 to 20 Hz. The horizontal stabilizer motor, used for trim only, produced a maximum torque of ±3.884 N-m and deflected the surface at a rate of 0.06 deg/sec. The stabilizer was capable of travel from 10° trailing edge down to 5° trailing edge up with respect to the fuselage waterline.

For cable-mounted models, an electrical "umbilical" cable is required to connect model sensors to readout instrumentation. In order to keep the umbilical cable small and light, thereby minimizing its effect on model response, the power to the onboard instrumentation and control actuator motors was supplied to the model through four copper-clad snubber cables.

A microelectronic multiplexing system was used to transmit electrical commands to the onboard instrumentation and to receive data signals from the model sensors simultaneously through the 0.159-cm-diameter coaxial umbilical cable. The details of the microelectronic system are given in the appendix. This system was capable of transmitting 10 channels of analog data simultaneously from the transducers within the model through the coaxial umbilical cable to the control room outside the test section. In addition, through this coaxial cable, the system could simultaneously code gain and offset commands to the onboard signal conditioning units, operate commands to the three control motors, and generate a timing signal for data synchronization.

ANALYTICAL MODEL RESPONSE STUDIES

Model Mount Effects

Analytical studies were conducted by the Boeing Company (Wichita Division) to determine the cable-mount effects on the model motions. The equations of motion and methods of analysis of reference 12 were used in the response studies. These studies consisted of comparisons of the response characteristics of the model when mounted on the flying cables and in free flight. In both cases, the measured vertical gust data shown in figure 4 were used in the analysis to generate spanwise gust loads on the model. In each case, the amplitude of the model response data was normalized by the averaged spanwise vertical gust angle $|\tilde{\epsilon}_g|$ indicated in figure 5(a). Typical results of this analysis are shown in figure 11 in terms of the variation with the reduced frequency k of the ratios $|C_n/\tilde{\epsilon}_g|$, $|C_q/\tilde{\epsilon}_g|$, $|C_b/\tilde{\epsilon}_g|$, and the associated phase angles. (See fig. 10 for measurement locations.) These results indicate that the mount has only a small effect on the model response at the reduced frequencies corresponding to the short-period ($k = 0.04$) and first elastic (wing-bending, $k = 0.072$) modes. A significant effect is indicated on the wing fore-and-aft bending mode (second elastic mode, $k = 0.14$). The sharp peak in the cable-mount data at low values of k ($k = 0.005$) is associated with the vertical translation mode of the model on the mount system and, hence, does not appear in the free-flight analysis.

Effect of Spanwise Variation of Gust Field on Analytically Derived Frequency Responses of Cable Mounted Model

Ideally, the gust field generated in the wind tunnel should be nearly uniform, but the tunnel measurements in figure 4 show that the gust amplitude apparently has significant spanwise variation. Therefore, it was decided to determine the difference between the theoretical model response caused by the measured tunnel gust distribution and that resulting from a uniform gust obtained by averaging the measurements across the span. The power spectral density approach (ref. 1) was used in the response calculations. This approach provides statistical descriptions of the dynamic response from a combination of power spectral description of the turbulent velocities with solutions of linear equations of motion for the airplane. Typical comparisons of results of the analysis using the measured tunnel gust distribution $|\epsilon_g|$ (replotted from fig. 11) and those caused by a uniform gust distribution $|\bar{\epsilon}_g|$ are shown in figure 12. This comparison shows that the spanwise gust variations in the tunnel have only a small effect (about 4 percent maximum) on the model response except at reduced frequencies above $k = 0.14$. The phase angles for the uniform gust field were calculated by using the cross-spectra between the turbulence input at the tunnel streamwise station corresponding to the location of the model c.g. and the response of the model. The data from figure 12 showing model response indicate that the gust in the tunnel can be considered uniform along the span. The insensitivity of the model response to the spanwise variable gust amplitude is probably a result of the nearly constant spanwise phase difference (fig. 4(b)).

Modeling of Atmospheric Turbulence

Atmospheric turbulence has been found to be essentially homogeneous and, therefore, with respect to the axes of an airplane in level flight, the turbulence gust velocities would be expected to vary along the span of the airplane as well as along the direction of flight. However, the most commonly used formulation of the spectral approach to calculating airplane response to turbulence has assumed a one-dimensional or "uniform" gust field. In this formulation the gust velocities are considered to vary randomly in the direction of flight but are uniform along the span. For an airplane with a large wing span (greater than about 5 percent of the turbulence scale), such as the B-52E, the one-dimensional analysis may not be sufficient. For this case, a more adequate gust model is obtained by assuming the turbulence to be a random two-dimensional isotropic gust (refs. 13 and 14). Furthermore, the analyses of reference 15 indicate that the two-dimensional gust analysis produces calculated airplane responses which more nearly agree with flight test results than does the one-dimensional analysis. Because the model response in the tunnel approximates that from a one-dimensional gust field (see fig. 12), it was desirable to determine the differences between the model response to one-dimensional and two-dimensional gust inputs. (The two-dimensional gust input of refs. 13 and 14 was used for these calculations.) If these differences are sufficiently large, then corrections which include these differences, plus corrections for the slight differences between the one-dimensional analysis and the response result-

ing from tunnel gusts (fig. 12) and the cable-mount effects (fig. 11), should be applied to the wind-tunnel data before comparisons with the flight test data can be made. Typical comparisons between the one- and two-dimensional random gust inputs for the model are shown in figure 13. These data show that the two-dimensional gust analysis gives peak values for the first elastic mode (i.e., $k \approx 0.07$) which are about 10 percent lower than those from the uniform analysis. This difference, when added to the difference in the responses of the model caused by the tunnel gust and the uniform (one-dimensional) analysis (fig. 12) and to the difference caused by cable-mount effects (fig. 11), gives maximum correction factors of approximately 12 percent for the reduced frequency range of interest (i.e., $0.01 \leq k \leq 0.14$). A comparison of the phase angles in figures 11 to 13 indicate that no corrections in phase angle are apparently necessary, except for the cable-mount effects at low reduced frequency ($k < 0.01$) in figure 11 and for cable and tunnel spanwise variation effects at the second elastic mode frequency ($k = 0.14$).

RESULTS AND DISCUSSION

Measured and Calculated Model Response

The model response to the gusts generated by oscillating the gust vanes over a range of frequencies at a tunnel flow velocity of 35.4 m/sec was measured in terms of accelerations and moments experienced by the model. A comparison of the uncorrected measured and the calculated frequency responses (fig. 12) of the model are shown in figure 14. (Note scale change relative to previous figures.) The nondimensional response coefficients of acceleration, pitching moment, and bending moment at various stations on the model are plotted in this figure. For the locations of the response stations, refer to figure 10. All data are for symmetric response with the model on the cable-mount system.

In general, the measured results agree well with calculated data, except at the higher reduced frequencies $k > 0.12$. The low gust level produced at the higher values of k undoubtedly resulted in inaccuracies in the measurement both of the response and the gust amplitudes. The analysis tends to predict a higher response than was measured for the first elastic mode ($k = 0.072$) for the acceleration at the fuselage aft end (fig. 14(c)), the pitching moment at the c.g. (fig. 14(d)), and the bending moments along the wing (figs. 14(e) and 14(f)).

The measured results shown in figures 14(b) and 14(d) show the repeatability of the gust response tests for two different runs (i.e., runs 1 and 2). For values of k below 0.16, the repeatability is excellent.

Model and Flight Test Results

The measured model and airplane flight test results are compared in figure 15. Two different sets of model data are presented - the "uncorrected" data from figure 14 and the "corrected" data, which have been adjusted to account for the cable-mount and two-dimensional gust effects.

The model and flight test data shown in figure 15 generally agree well for values of reduced frequencies from 0.03 to 0.14, which include the short-period and first elastic modes. However, the pitching-moment data (fig. 15(d)) do not agree well, and much scatter appears in the flight data for $k > 0.08$. It should be noted that at low reduced frequencies ($k < 0.03$), all the airplane data were affected by spurious pilot-induced motions (ref. 15). Also, at the higher reduced frequencies ($k > 0.14$), the low gust level produced by the airstream oscillator led to measurement errors in the model data. The short-period mode of motion ($k \approx 0.04$) did not show up very well in either the flight test or model response data. At best, it can barely be detected in the model data of figure 15. On the whole, it is completely overpowered by the strong first elastic mode. This illustrates the high degree of flexibility in the B-52E airplane structure.

The major difference noted between corrected and uncorrected model data is that corrections reduce the peak amplitude of the first elastic mode of the model ($k = 0.072$) by about 10 percent. The result is better agreement with the flight data. The correction improved the phase angle and, in most cases, the coefficient amplitudes associated with the low-frequency cable mode ($k \approx 0.01$); however, in general, the corrections produced only minor changes in the results.

CONCLUDING REMARKS

A wind-tunnel technique for obtaining gust frequency-response functions for use in predicting the response of flexible aircraft to atmospheric turbulence has been evaluated by comparing the tunnel test results for a dynamically scaled cable-supported aeroelastic model of the B-52E airplane with analytical and flight data.

These studies show good correlation between wind-tunnel, flight test, and analytical predictions for the short-period and first elastic modes of motion. Since these two modes are generally the ones primarily associated with aircraft gust response, the good correlation of results for these modes in the present study indicates that the wind-tunnel/airstream oscillator technique should be a useful and valid tool for evaluating gust response characteristics of airplanes.

Langley Research Center
National Aeronautics and Space Administration
Hampton, VA 23665
September 24, 1979

APPENDIX

MICROELECTRONIC INSTRUMENTATION SYSTEM

A block diagram of the microelectronic system used in the B-52E model wind-tunnel gust tests is presented in figure 16. Both the instrumentation components located onboard the model and those located in the control room are shown. The connecting links between the two locations are the coaxial umbilical cable, which carried signals from the transducers and transmitted commands to the trim control motors, and the four copper-clad snubber cables which carried the power to the onboard instrumentation.

The instrument components located in the model (see fig. 16) consisted of 10 transducers, a transducer selector switch, 2 FM data modulators, a switch control unit, a receiver decoder unit, and 6 dc-dc voltage converters. Each of the two data modulator units contained five voltage-controlled FM oscillators; thus, each could handle five incoming transducer signals simultaneously. In addition, a remotely operated transducer selector unit (see fig. 16), which allowed time-sharing signals, was used with data modulator B; thus, this modulator unit could handle selectively a total of 10 transducer signals, 5 at a time. The transducer selector unit and the control surface motors were controlled by the switch control unit. Regulated power was supplied to each of the transducers and other onboard instrumentation by the onboard power converters. The arrangement of onboard instrumentation in the model is indicated in figure 17.

The control room instrumentation used in the model tests (refer to fig. 16) consisted of a two-way multicoupler, a group carrier converter, an analog tape recorder, a demodulator, a display and control panel, a control code generator, and a control signal modulator. The display and control panel contained a set of miniature oscilloscopes for continuous monitoring of each data channel and a control panel for changing channel gains and offsets. The model trim control signals for the stabilizer and aileron control surfaces were also routed through the display and control panel. The signals to and from the oscillating vane system were also passed through the microelectronic system, as shown at the top of figure 16. This allowed the oscillating vane data to be time-synchronized with the model response data on the analog tape.

REFERENCES

1. Houbolt, John C.; Steiner, Roy; and Pratt, Kermit G.: Dynamic Response of Airplanes to Atmospheric Turbulence Including Flight Data on Input and Response. NASA TR R-199, 1964.

2. Pratt, Kermit G.: Response of Flexible Airplanes to Atmospheric Turbulence. Performance and Dynamics of Aerospace Vehicles, NASA SP-258, 1971, pp. 439-503.

3. Coleman, Thomas L.; Murrow, Harold N.; and Press, Harry: Some Structural Response Characteristics of a Large Flexible Swept-Wing Airplane in Rough Air. J. Aero. Sci., vol. 25, no. 8, Aug. 1958, pp. 515-521, 536.

4. Bennett, Floyd V.; and Pratt, Kermit G.: Calculated Responses of a Large Sweptwing Airplane to Continuous Turbulence With Flight-Test Comparisons. NASA TR R-69, 1960.

5. Coleman, Thomas L.; Press, Harry; and Meadows, May T.: An Evaluation of Effects of Flexibility on Wing Strains in Rough Air for a Large Swept-Wing Airplane by Means of Experimentally Determined Frequency-Response Functions With an Assessment of Random-Process Techniques Employed. NASA TR R-70, 1960. (Supersedes NACA TN 4291.)

6. Chernoff, Max; and Rothman, Herbert L.: Unsteady Frequency Response Functions for Use in Power Spectral Analysis. J. Aerosp. Sci., vol. 29, no. 2, Feb. 1962, pp. 121-129.

7. Zbrozek, J. K.: Longitudinal Response of Aircraft to Oscillatory Vertical Gusts (Frequency Analysis Including the Effect of Unsteady Aerodynamics). Rep. No. Aero.2559, British R.A.E., Nov. 1955.

8. Reed, William H., III; and Abbott, Frank T., Jr.: A New "Free-Flight" Mount System for High-Speed Wind-Tunnel Flutter Models. Proceedings of Symposium on Aeroelastic & Dynamic Modeling Technology, RTD-TDR-63-4197, Pt. I, U.S. Air Force, Mar. 1964, pp. 169-206.

9. Gilman, Jean, Jr.; and Bennett, Robert M.: A Wind-Tunnel Technique for Measuring Frequency-Response Functions for Gust Loads Analyses. J. Aircr., vol. 3, no. 6, Nov.-Dec. 1966, pp. 535-540.

10. Rainey, A. Gerald; and Abel, Irving: Wind-Tunnel Techniques for the Study of Aeroelastic Effects on Aircraft Stability, Control, and Loads. Aeroelastic Effects From a Flight Mechanics Standpoint, AGARD CP No. 46, Mar. 1970, pp. 18-1 - 18-15.

11. Harder, Robert L.; and Desmarais, Robert N.: Interpolation Using Surface Splines. J. Aircr., vol. 9, no. 2, Feb. 1972, pp. 189-191.

12. Gilley, T. A.: B-52 Aeroelastic Model - Summary Report. D3-7763-1 (Contract No. F33615-67-C-1264), Boeing Co., Apr. 25, 1968.

13. Sawdy, David T.: On the Two-Dimensional Atmospheric Turbulence Response of an Airplane. Ph. D. Diss., Univ. of Kansas, 1966. (Available as NASA CR-91116.)

14. Pratt, Kermit G.: Effect of Spanwise Variation of Turbulence on the Normal Acceleration of Airplanes With Small Span Relative to Turbulence Scale. NASA TM X-72748, 1975.

15. Gilley, T. A.; and Cast, Rudy D.: B-52C-F Dynamic Responses and Load Survey (Volume II) - WFT 1293 (Volume II - Theoretical and Experimental Frequency Response Function Comparisons). Doc. No. D3-7060-2 (Contract No. AF34(601)-17947), Boeing Co., Sept. 27, 1966. (Available from DDC as AD 904 598.)

TABLE I.- MODEL SCALE FACTORS

Scaled quantity	Formula	Factor
Reduced frequency	$\frac{l_M}{l_A}\frac{\omega_M}{\omega_A}\frac{V_A}{V_M}$	1.0
Froude number	$\frac{V_M}{V_A}\left(\frac{l_A}{l_M}\frac{g_A}{g_M}\right)^{1/2}$	1.0
Mass ratio	$\frac{W_M}{W_A}\frac{\rho_A}{\rho_M}\left(\frac{l_A}{l_M}\right)^3$	1.0
Dimension	Selected	1/30
Fluid density	$\frac{\text{Tunnel} = 0.008}{\text{Airplane} = 0.0019634}$	4.07
Velocity	$\left(\frac{l_M}{l_A}\right)^{1/2}$	0.183
Dynamic pressure	$\frac{\rho_M}{\rho_A}\left(\frac{V_M}{V_A}\right)^2$	0.136
Frequency	$\frac{V_M}{V_A}\frac{l_A}{l_M}$	5.48
Weight	$\frac{\rho_M}{\rho_A}\left(\frac{l_M}{l_A}\right)^3$	0.000151

TABLE II.- COMPARISON BETWEEN MODEL AND AIRPLANE TEST CONDITIONS

Parameter	Airplane	Model
Altitude, m	1646	NA
Velocity, m/sec	193	35.4
Mach number	0.569	0.226
Dynamic pressure, Pa	18 826	2557
Temperature, K	286	300
Mass, kg	189 964	28.7
Density, kg/m^3	1.012	4.123
Speed of sound, m/sec	339	156
Flight environment	Air	Freon-12
Mean aerodynamic chord, m . . .	6.99	0.233
Wing span, m	56.39	1.88
Wing area, m^2	371.67	0.413
Center of gravity, m	F.S. 20.57	F.S. 0.6858

TABLE III.- SUMMARY OF MODEL FREQUENCIES

(a) Wind-off elastic symmetric modal frequencies

Mode	Frequency, Hz	
	Calculated	Measured (a)
1	3.12	3.45
2	6.90	6.75
3	8.82	8.75
4	10.68	10.65
5	11.06	11.45
6	11.12	11.70
7	14.13	14.65
8	16.43	17.35
9	17.69	17.85

[a]Model mounted on soft spring and flying cables.

(b) Wind-on rigid body frequencies

Mode	Frequency, Hz	
	Calculated	Measured (a)
Short period	0.15	0.24
Translation	1.85	1.93

[a]Model mounted on flying cables; V = 35.4 m/sec.

TABLE IV.- WIND-OFF CANTILEVERED NACELLE STRUT MODES

Mode, strut bending	Natural frequency, Hz			
	Inboard strut and nacelle		Outboard strut and nacelle	
	Design	Actual	Design	Actual (a)
Side	11.17	11.12	11.50	11.48
Vertical	22.29	21.62	22.02	21.86
Torsion	32.92	-----	32.92	-----

[a]Actual frequencies are average of left and right nacelle strut frequencies.

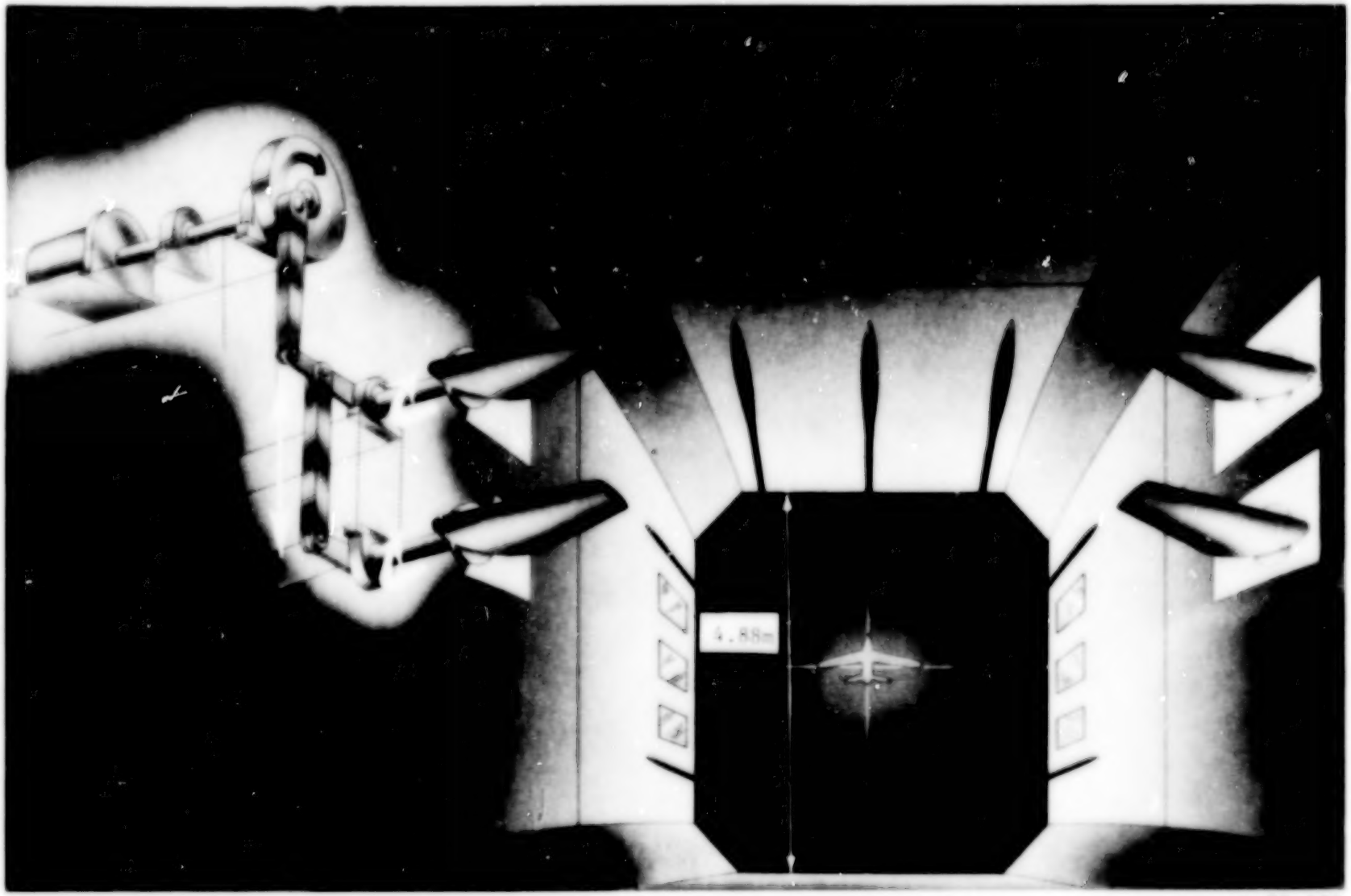

L-79-309

Figure 1.- View of airstream oscillator vane system in Langley transonic dynamics tunnel showing cutaway of mechanism.

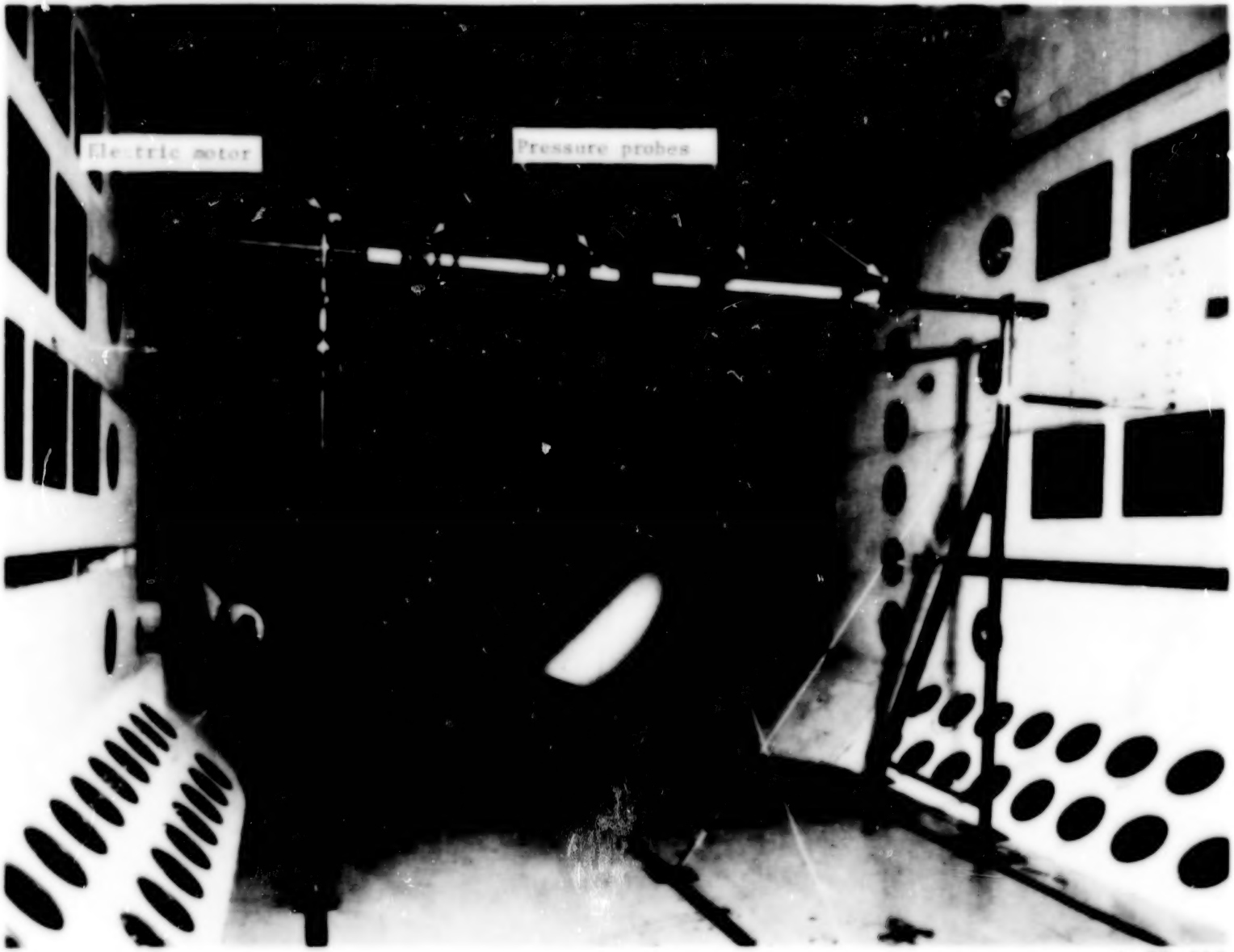

L-79-310

Figure 2.- Oscillating flow measurement probes mounted on motor driven traversable bar.

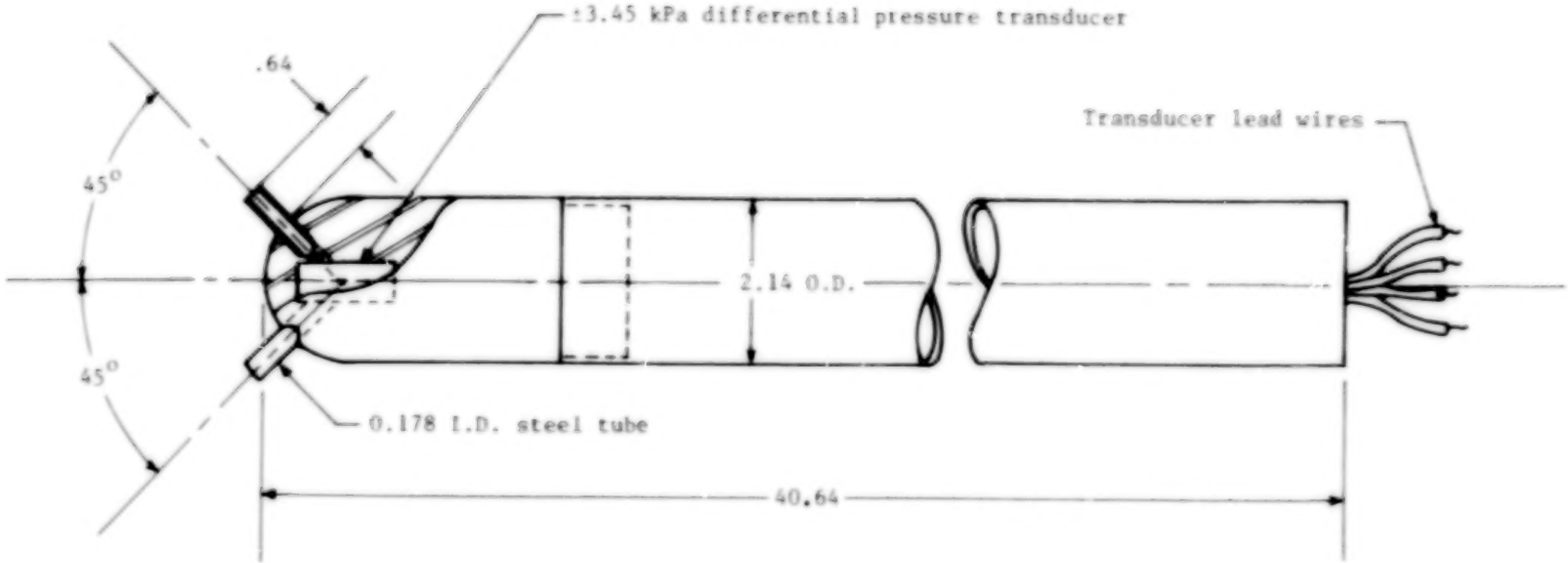

Figure 3.- Flow angle probe geometry. (Linear dimensions in cm; I.D. represents inner diameter; O.D., outer diameter.)

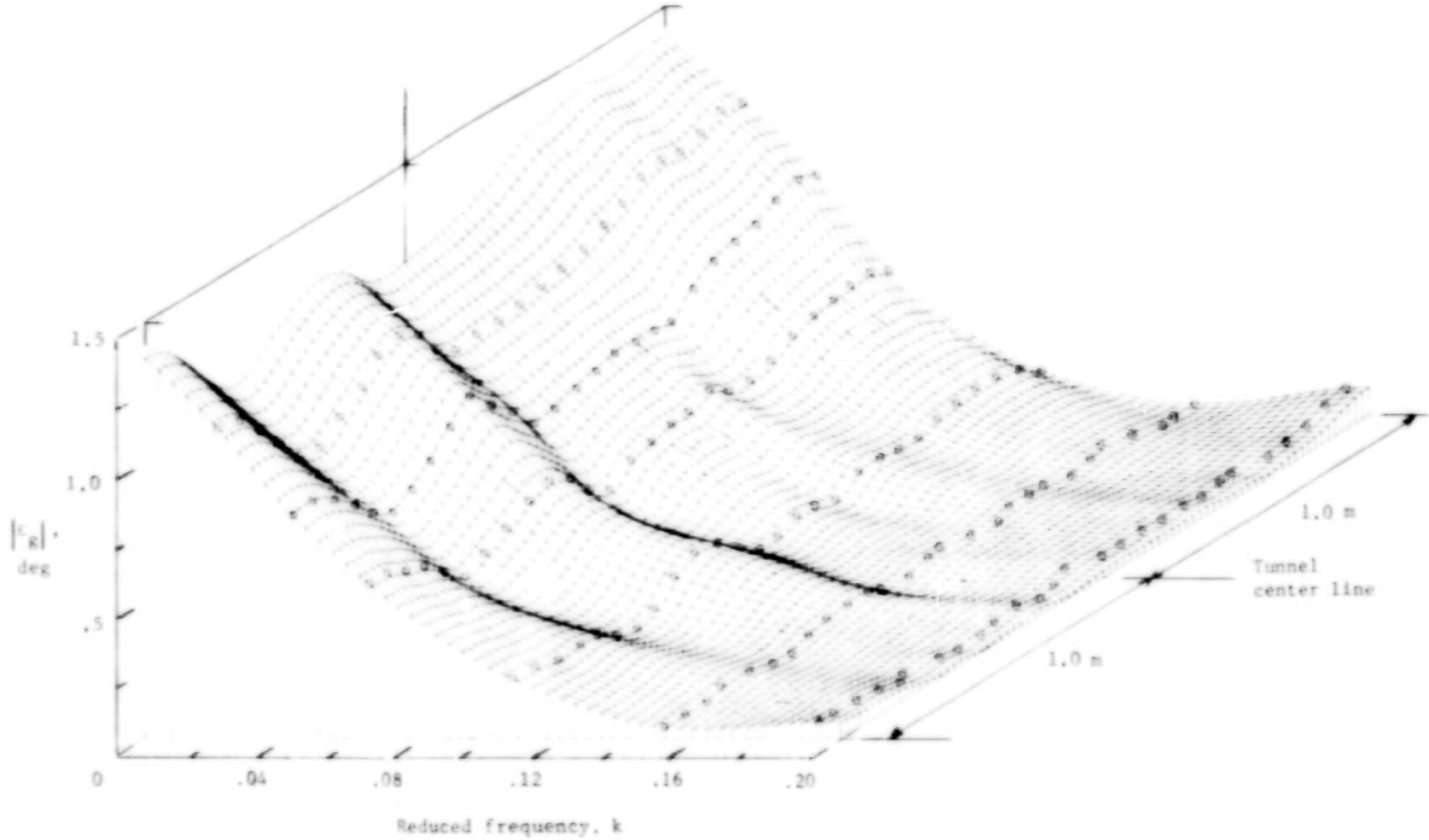

(a) Gust amplitude.

Figure 4.- Variation of amplitude and phase angle of gust flow with reduced frequency and lateral position. $\delta_v = \pm 6^o$; V = 35.4 m/sec; and $\bar{c}$ = 0.233 m.

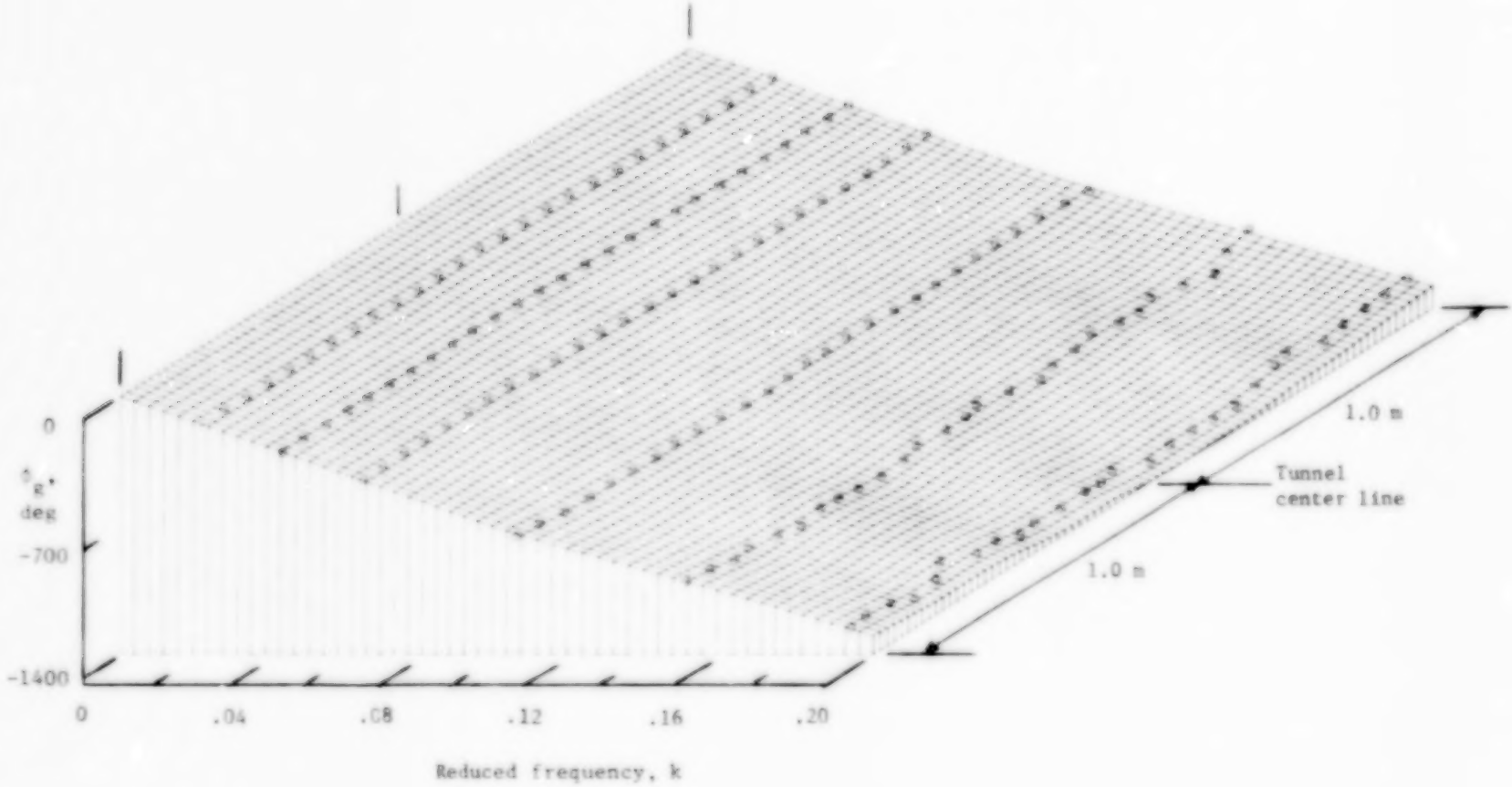

(b) Gust phase angle.

Figure 4.- Concluded.

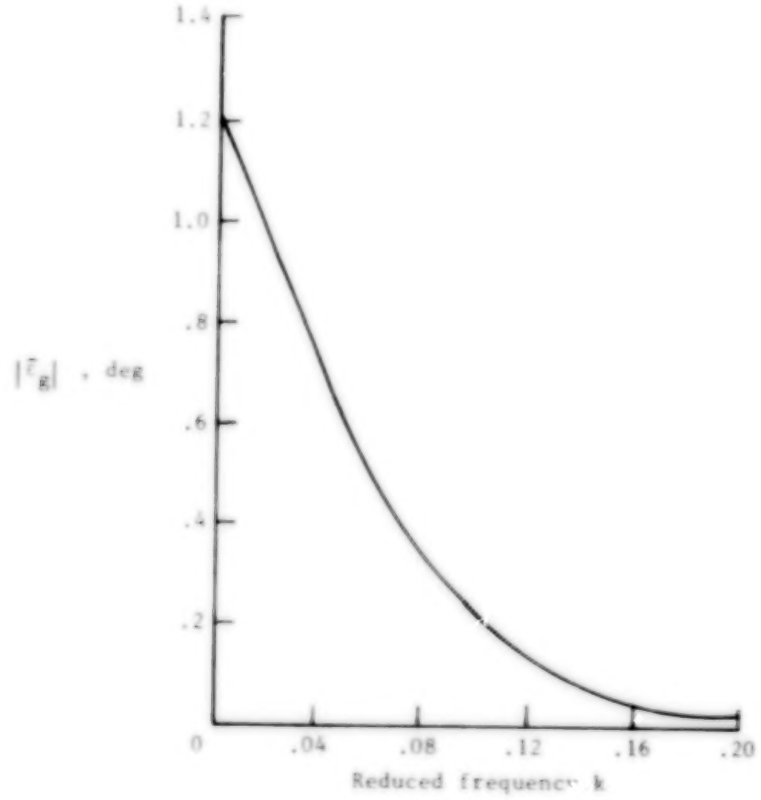

(a) Gust amplitude.

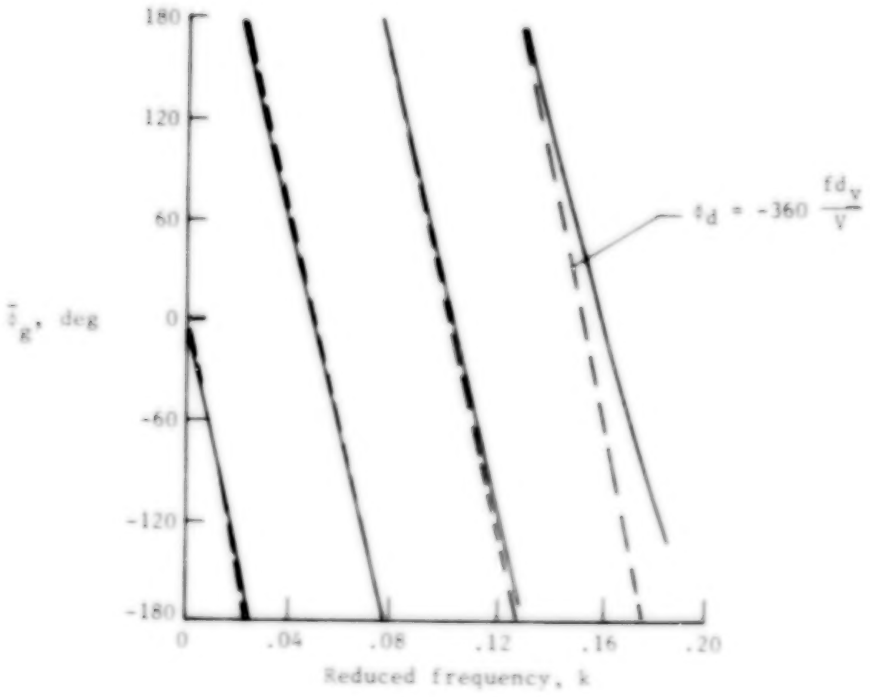

(b) Gust phase angle.

Figure 5.- Variation of averaged spanwise gust amplitude and phase angle with reduced frequency.

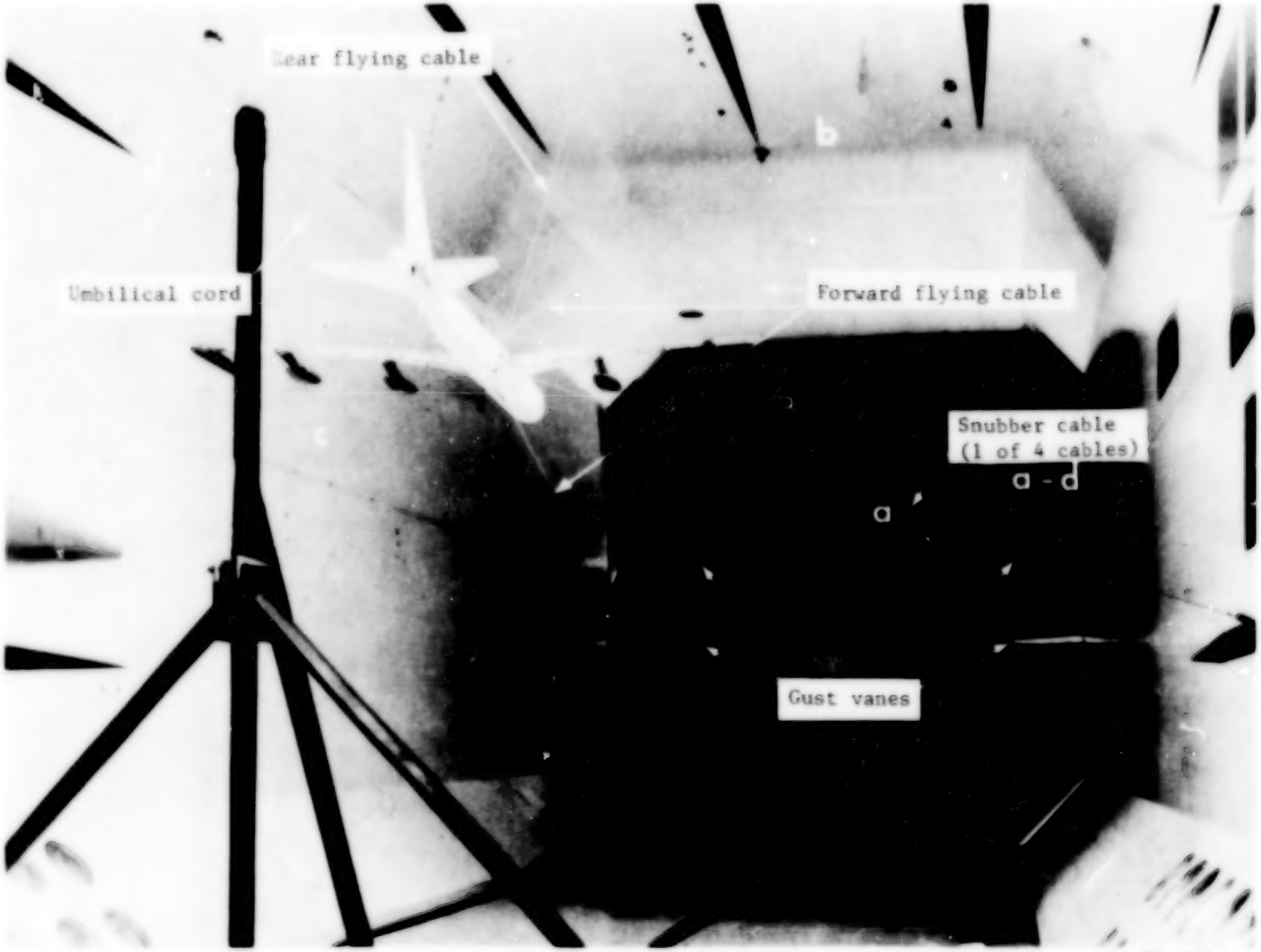

L-70-3779.1

Figure 6.- Model of B-52E airplane mounted in Langley transonic dynamics tunnel.

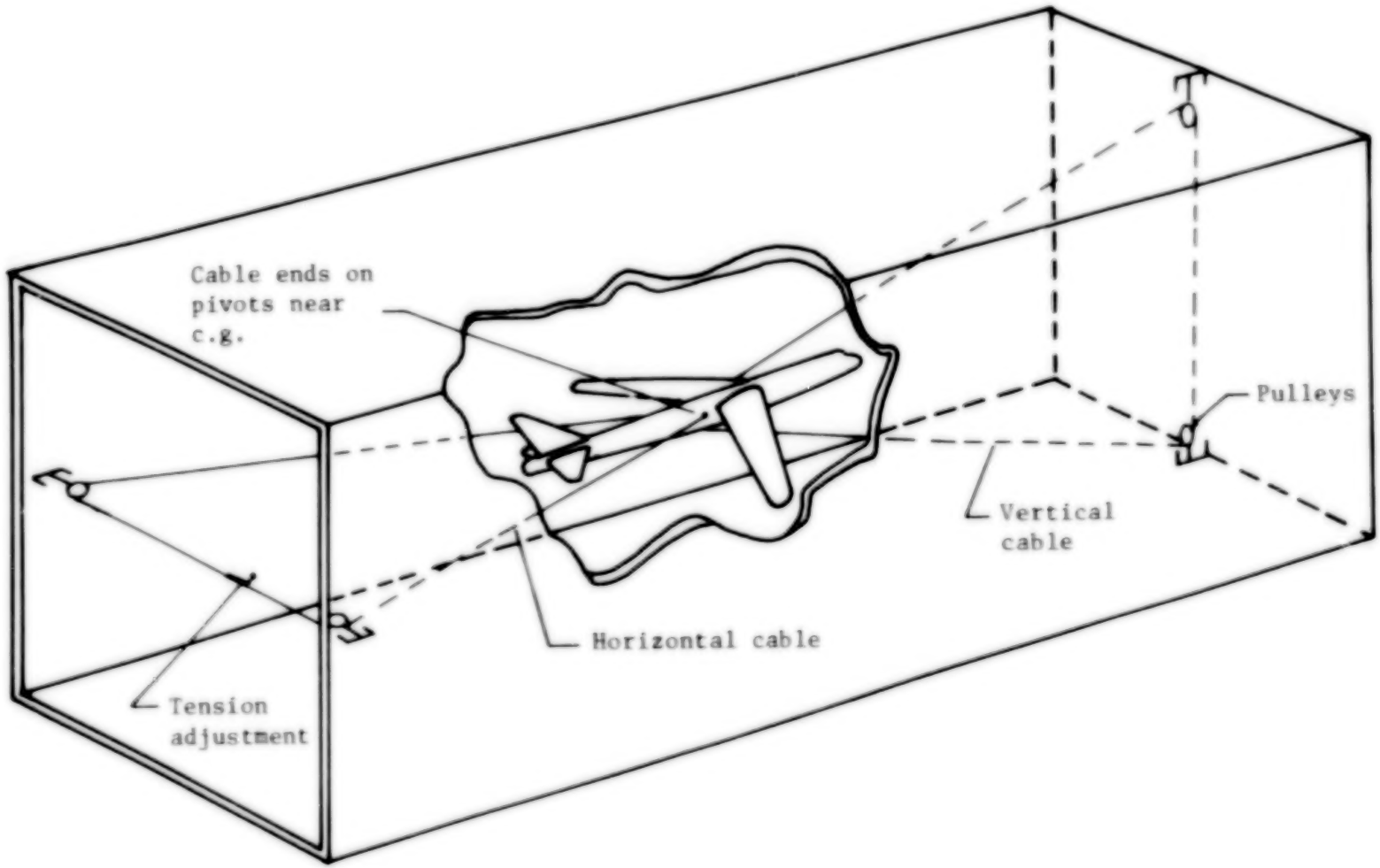

Figure 7.- Modified two-cable-mount system.

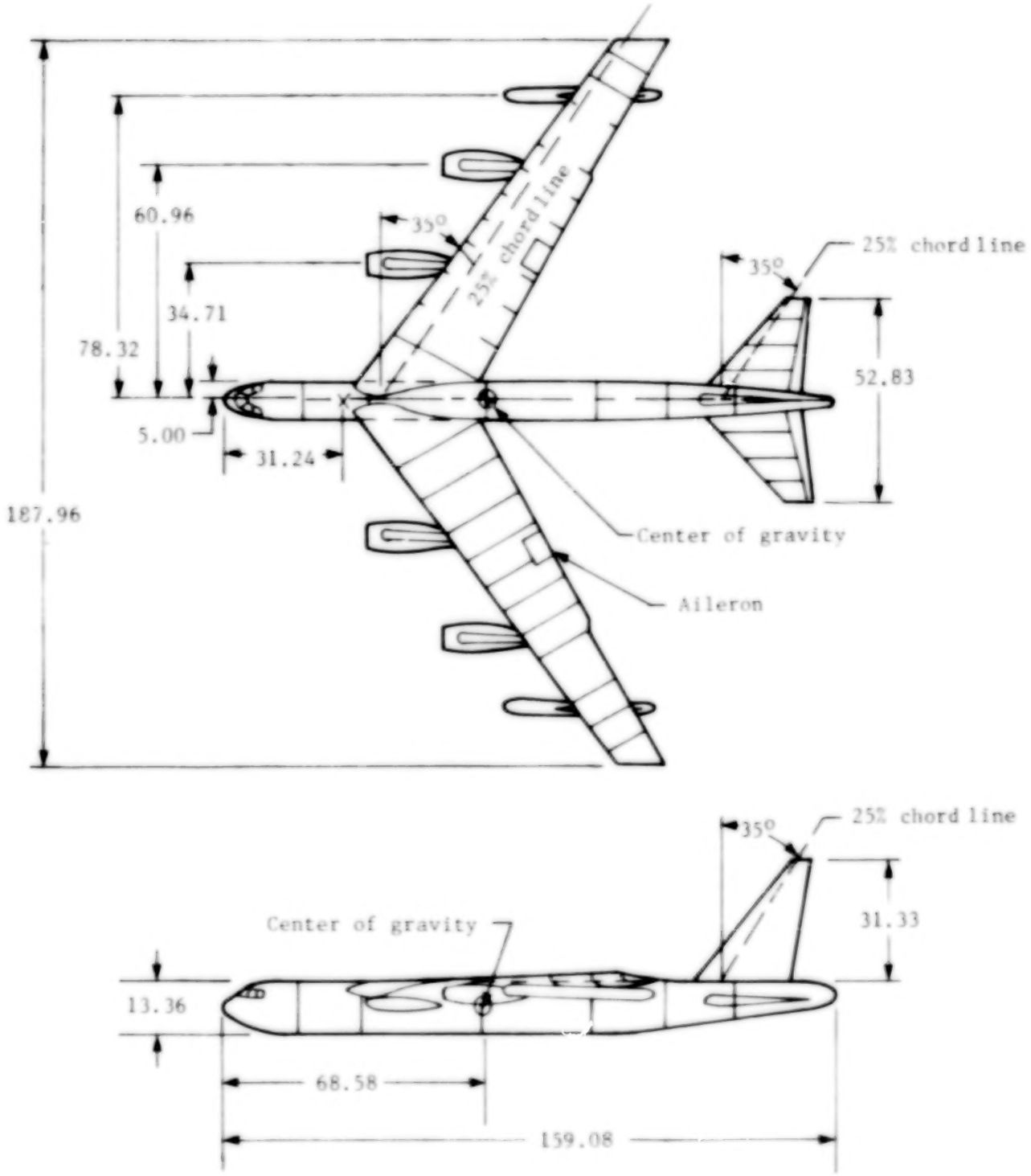

Figure 8.- Model geometry. (All linear dimensions are in cm.)

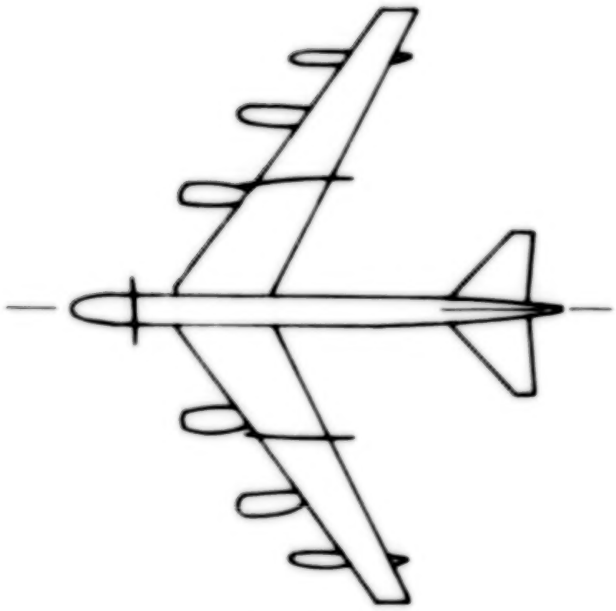

First elastic mode
(wing bending);
f = 3.45 Hz

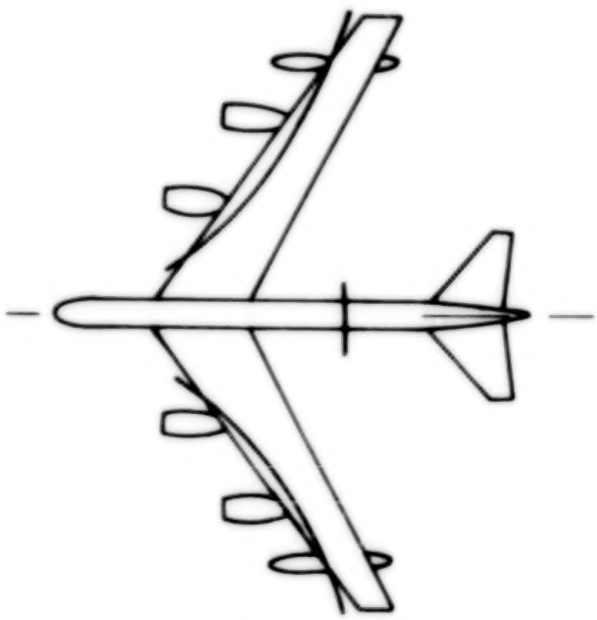

Second elastic mode
(wing fore and aft);
f = 6.75 Hz

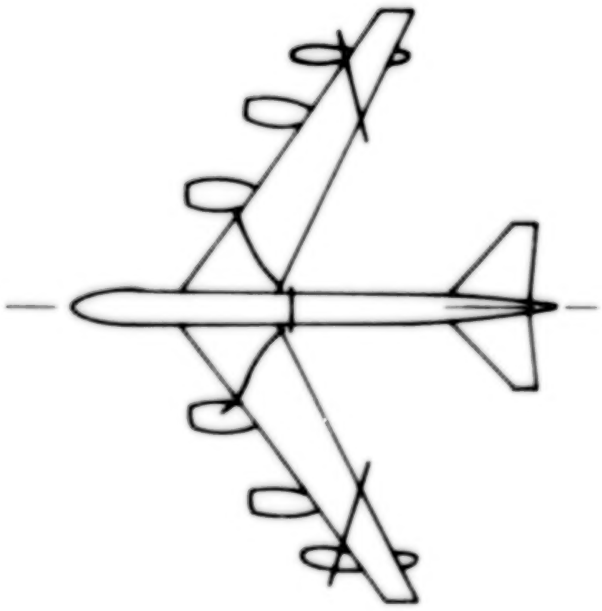

Third elastic mode;
f = 8.75 Hz

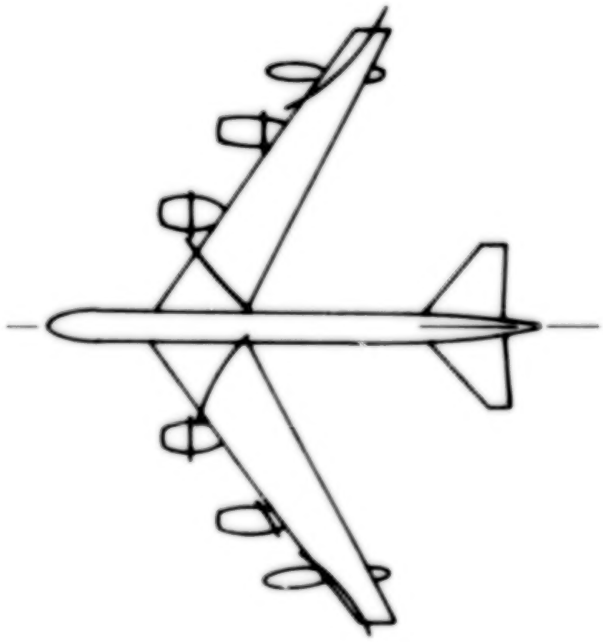

Fourth elastic mode;
f = 10.65 Hz

Figure 9.- Measured node lines for important symmetric structural modes of model.

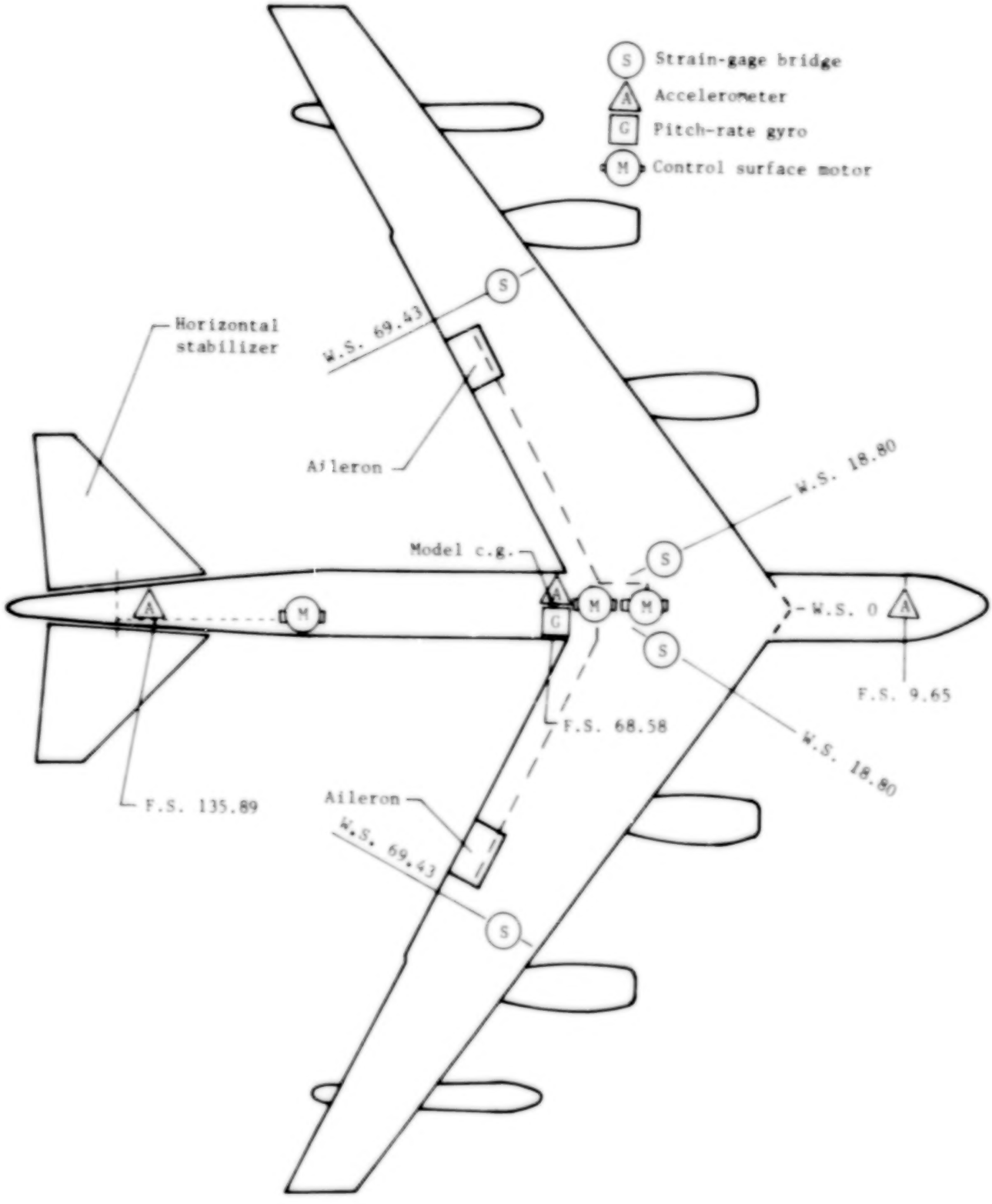

Figure 10.- Location of sensors and motors on model.

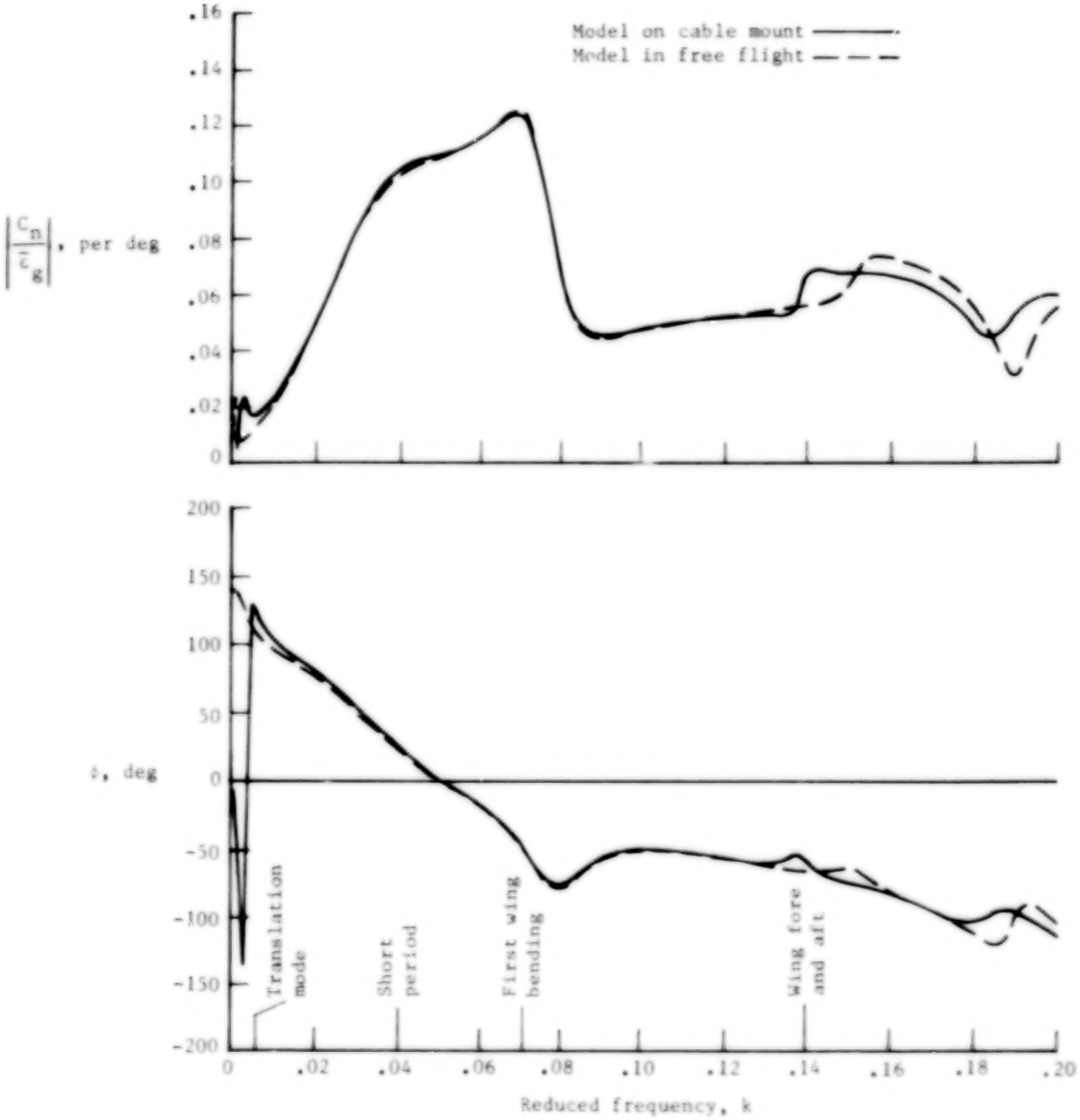

(a) Normal acceleration at fuselage station 68.58.

Figure 11.- Comparison of analytically derived model frequency-response characteristics for conditions of free flight and on cable mount.

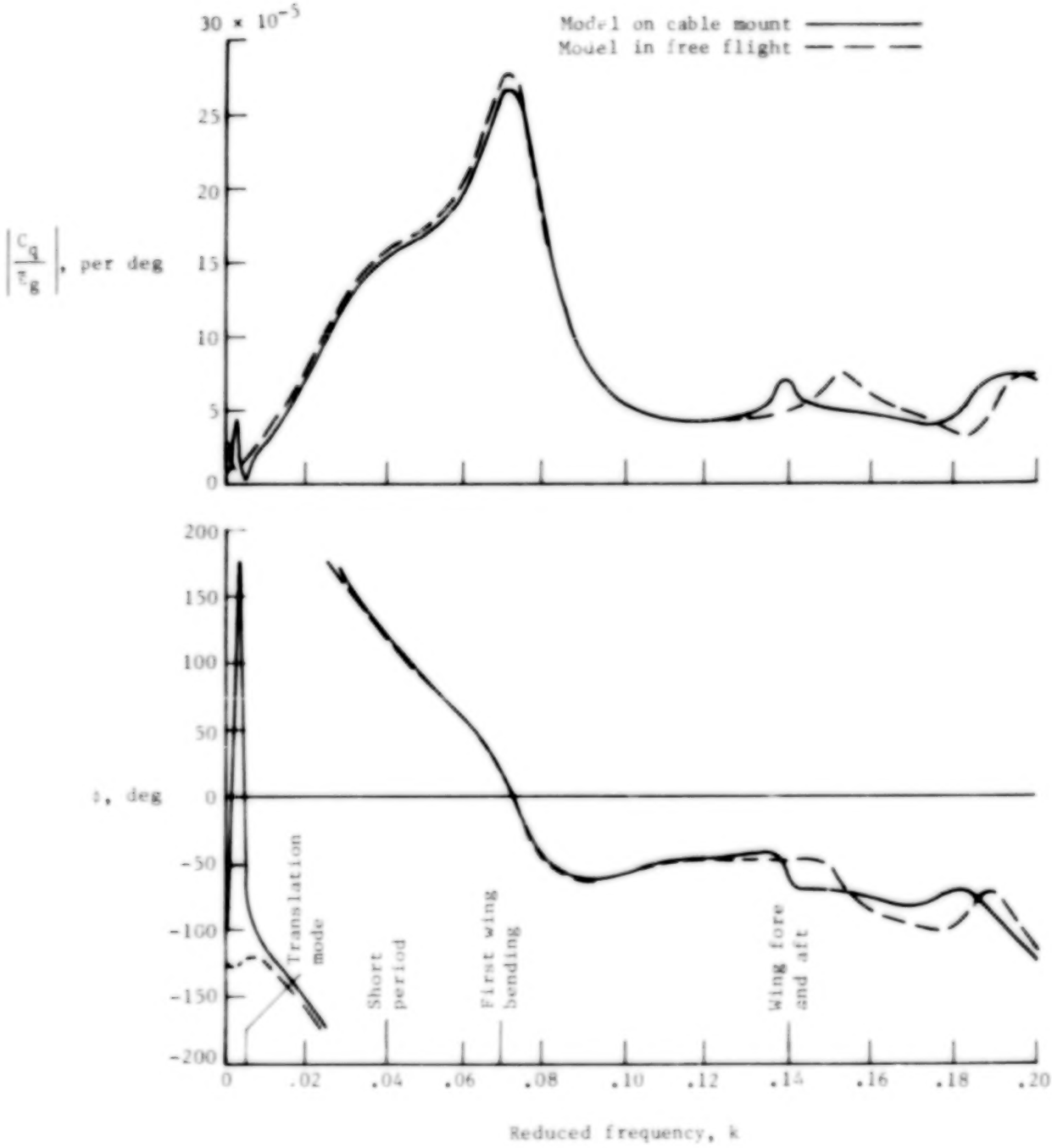

(b) Pitching moment at fuselage station 68.58.

Figure 11.- Continued.

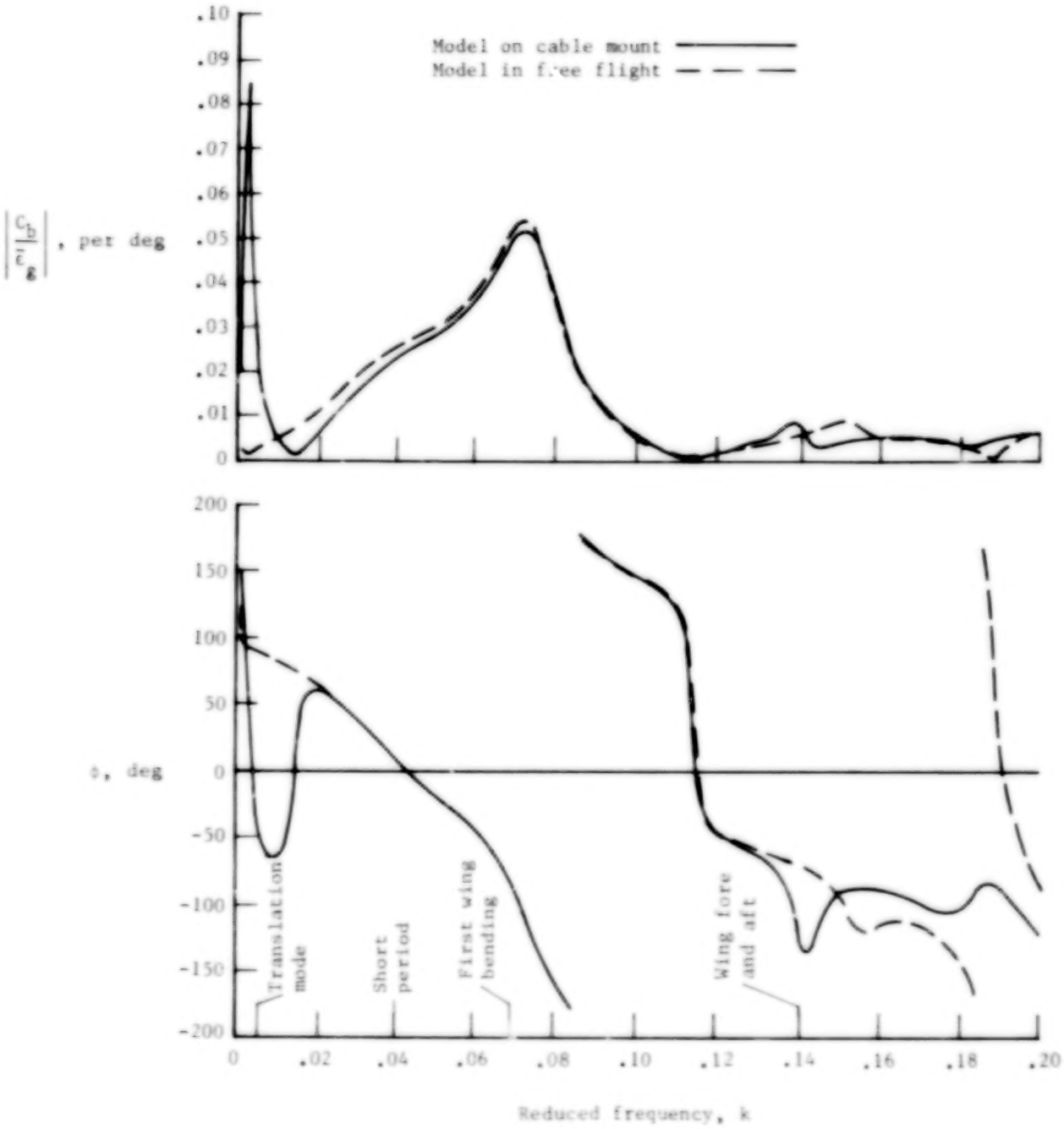

(c) Wing bending moment at wing station 18.80.

Figure 11.- Concluded.

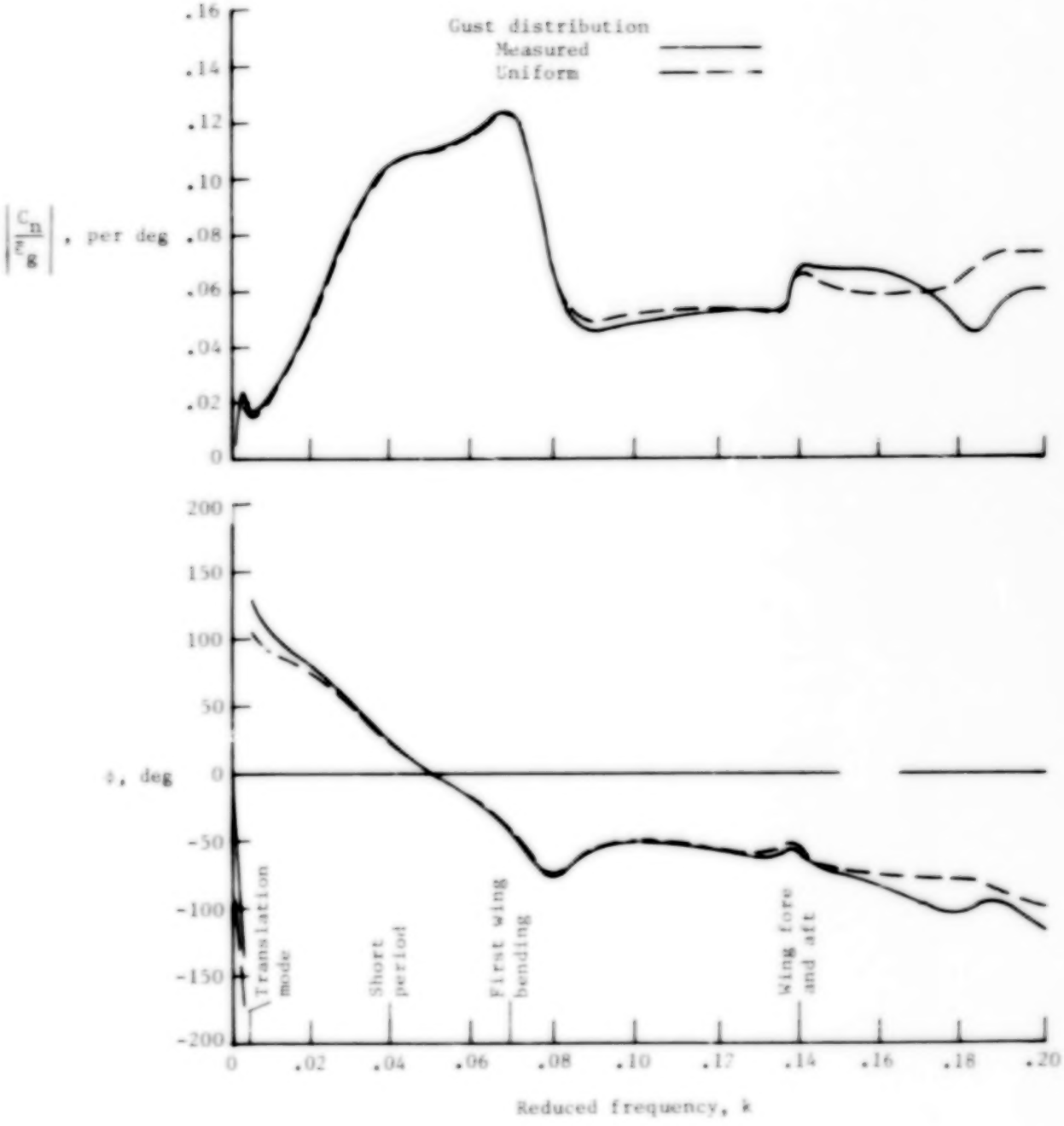

(a) Normal acceleration at fuselage 68.58.

Figure 12.- Comparison of analytically derived frequency-response characteristics of cable-mounted model for measured and uniform gust excitation.

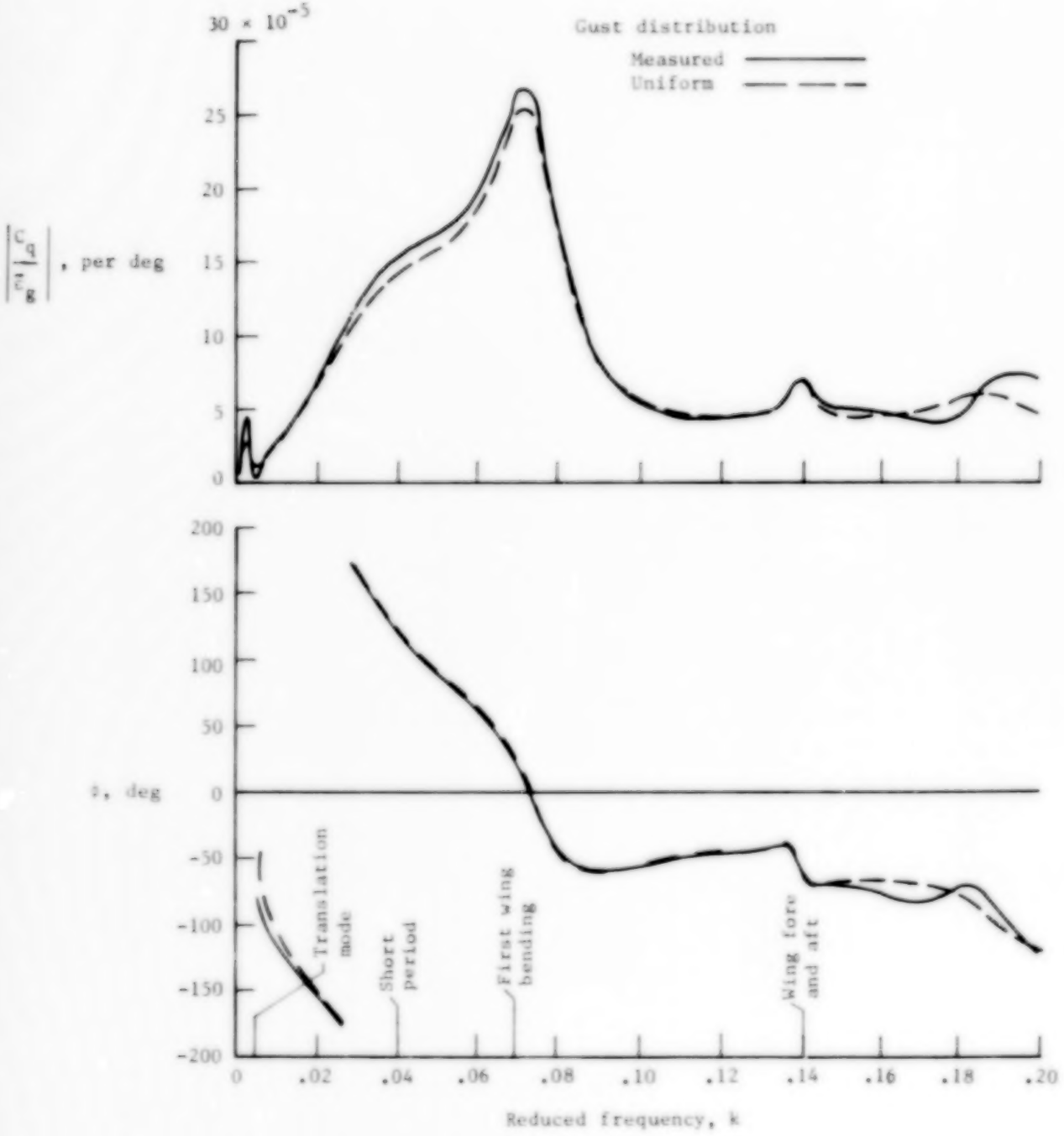

(b) Pitching moment at fuselage station 68.58.

Figure 12.- Continued.

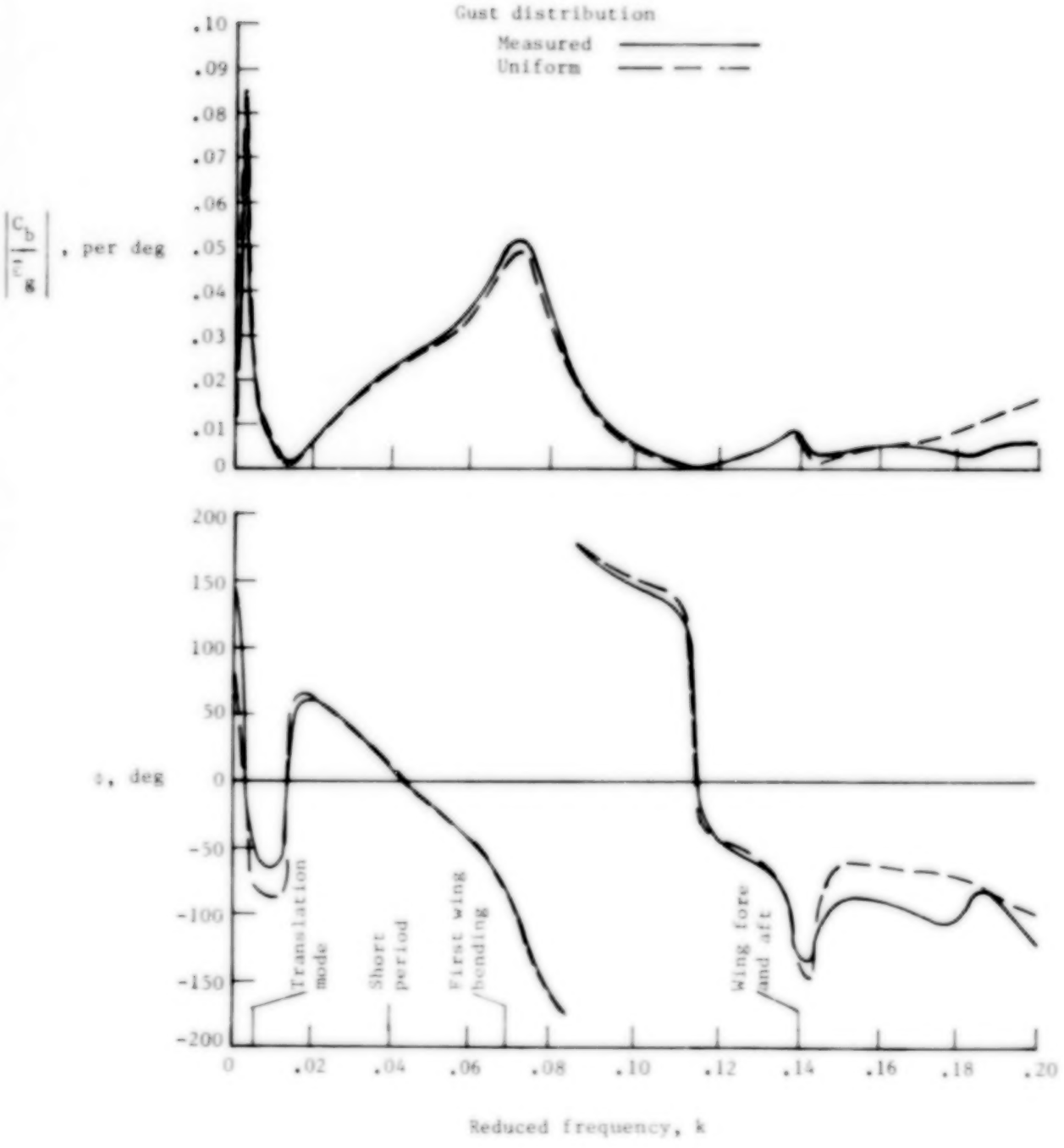

(c) Wing bending moment at wing station 18.80.

Figure 12.- Concluded.

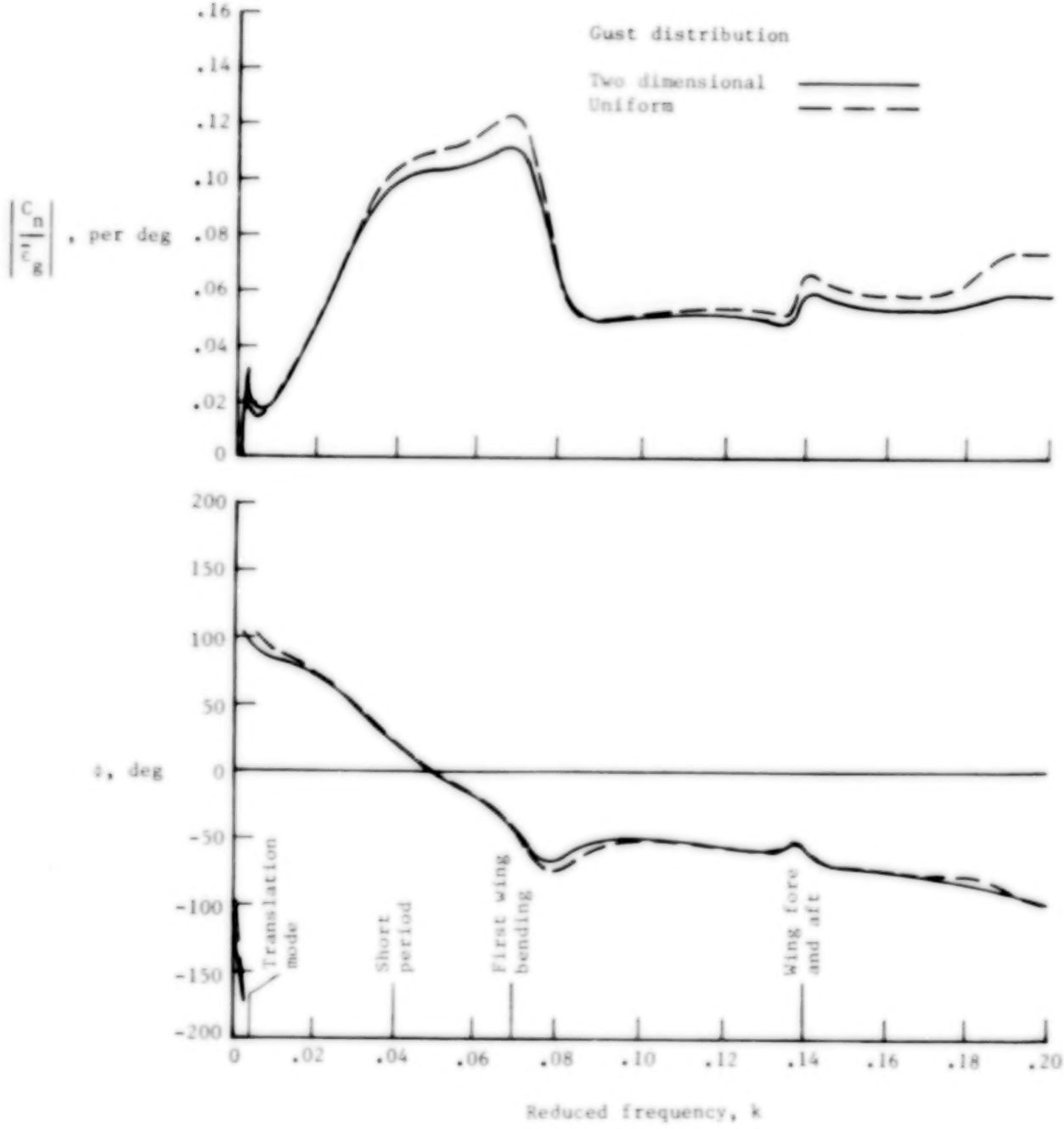

(a) Normal acceleration at fuselage station 68.58.

Figure 13.- Comparison of analytically derived frequency-response characteristics for two-dimensional and uniform gust excitation.

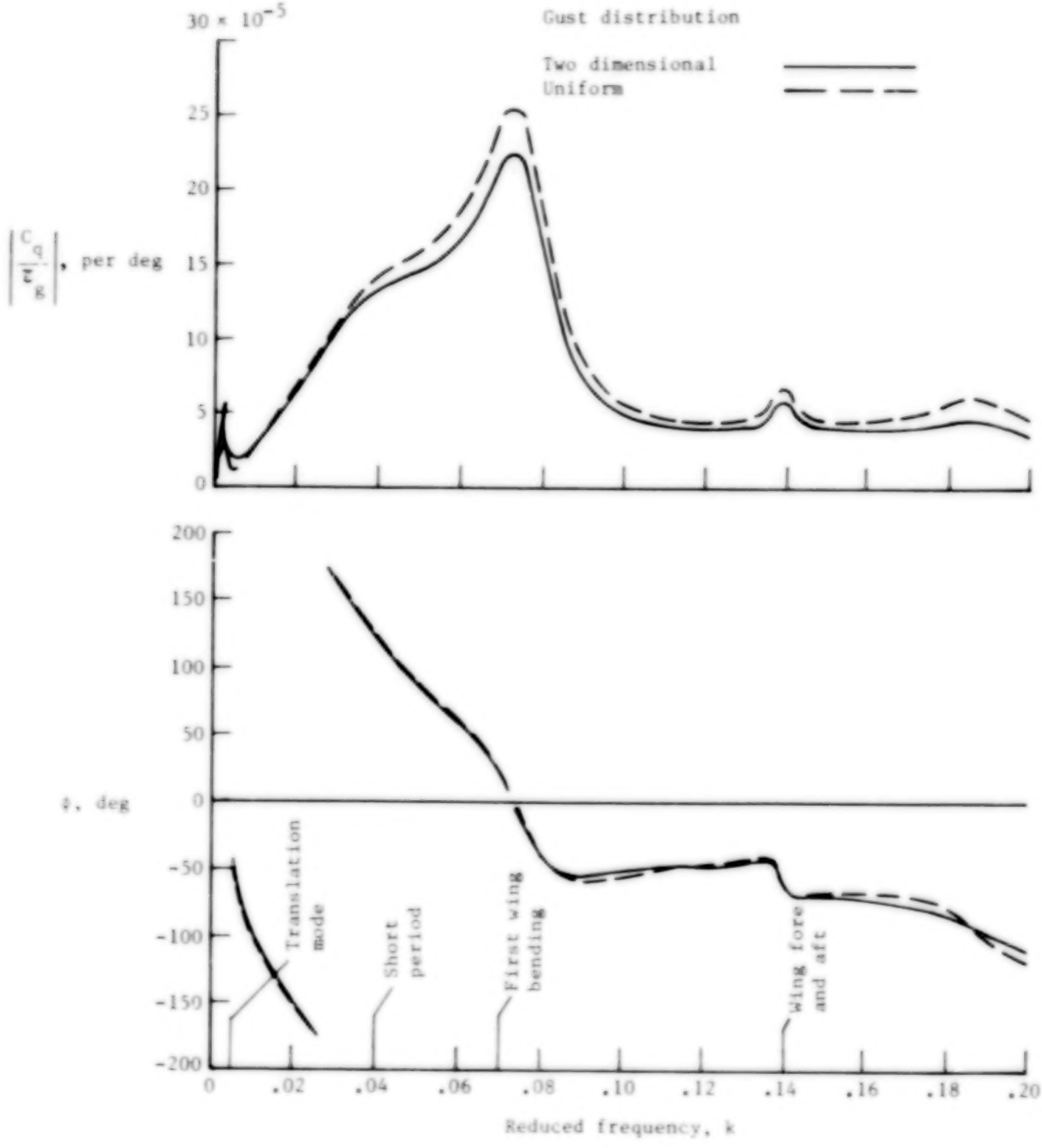

(b) Pitching moment at fuselage station 68.58.

Figure 13.- Continued.

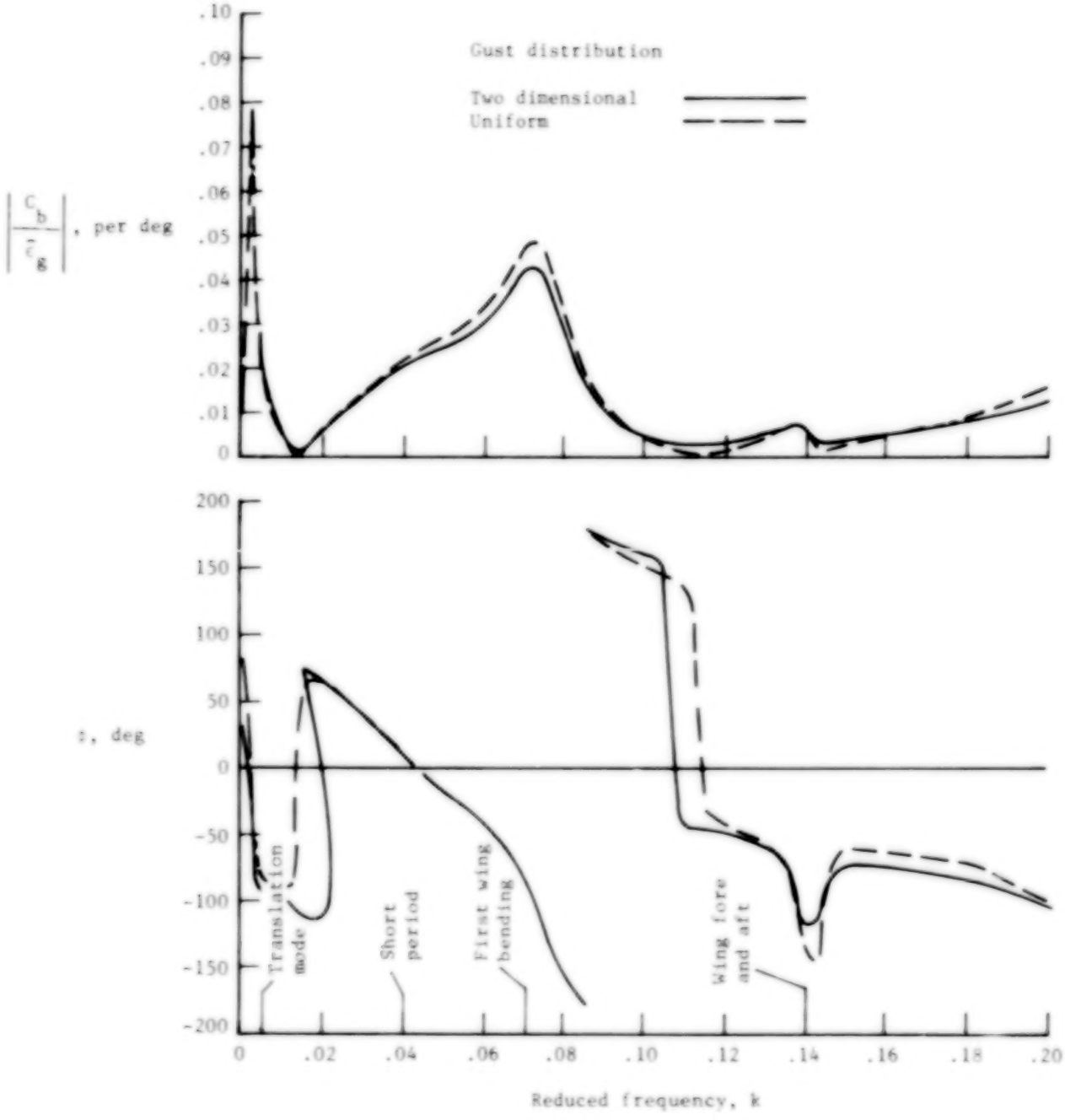

(c) Wing bending moment at wing station 18.80.

Figure 13.- Concluded.

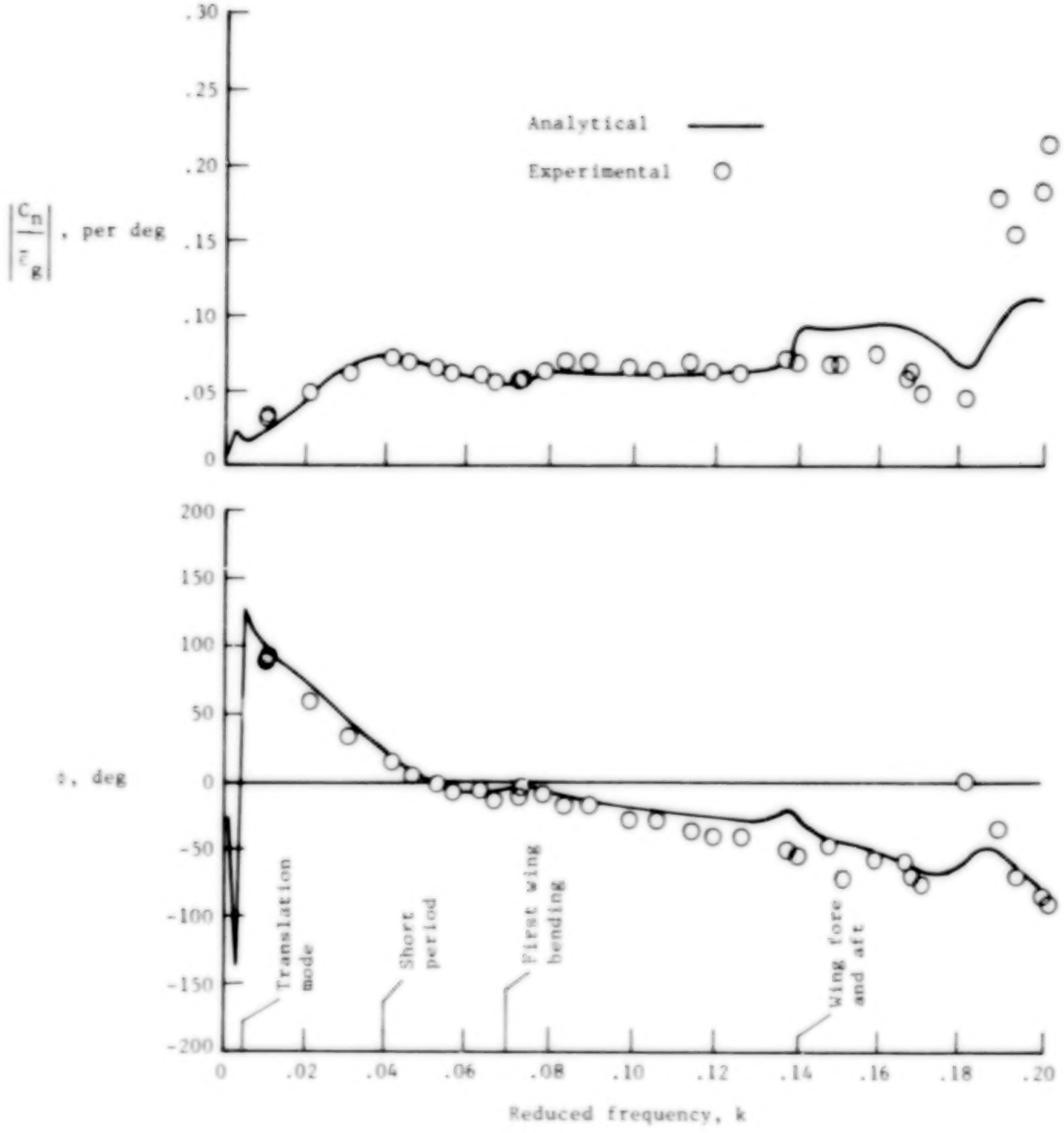

(a) Normal acceleration at fuselage station 9.65.

Figure 14.- Comparison of model uncorrected experimental and analytical frequency-response characteristics.

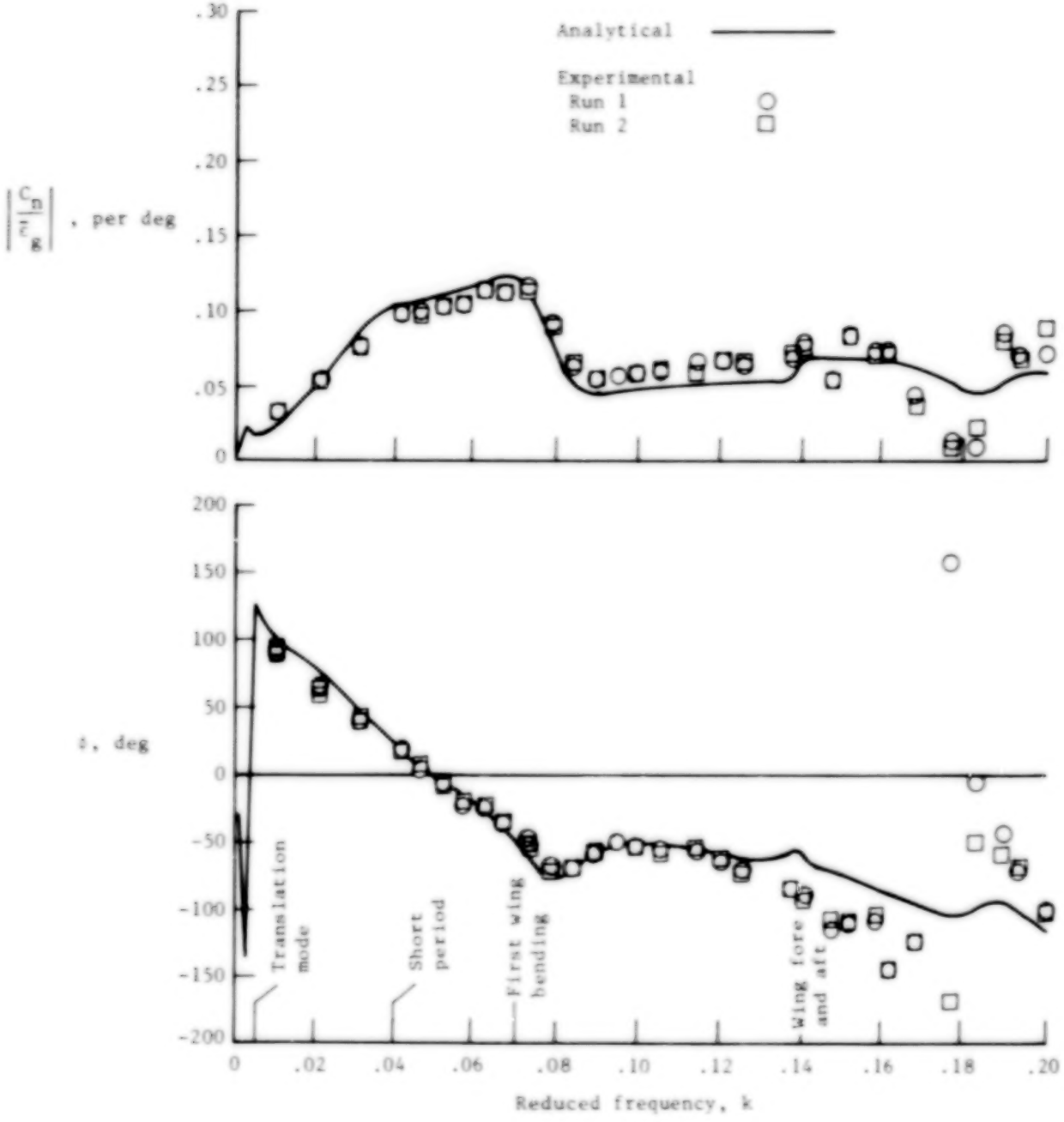

(b) Normal acceleration at fuselage station 68.58.

Figure 14.- Continued.

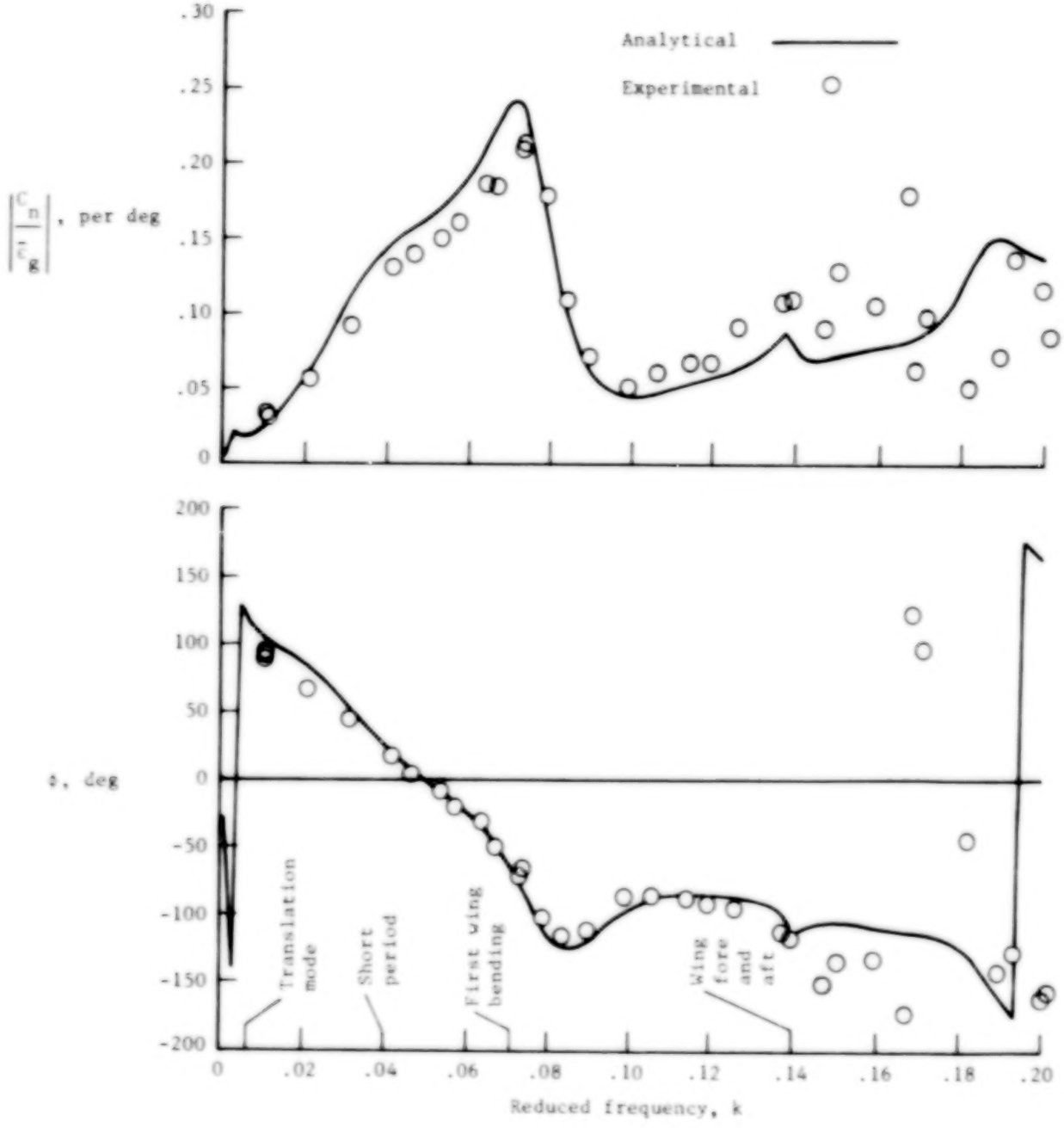

(c) Normal acceleration at fuselage station 135.89.

Figure 14.- Continued.

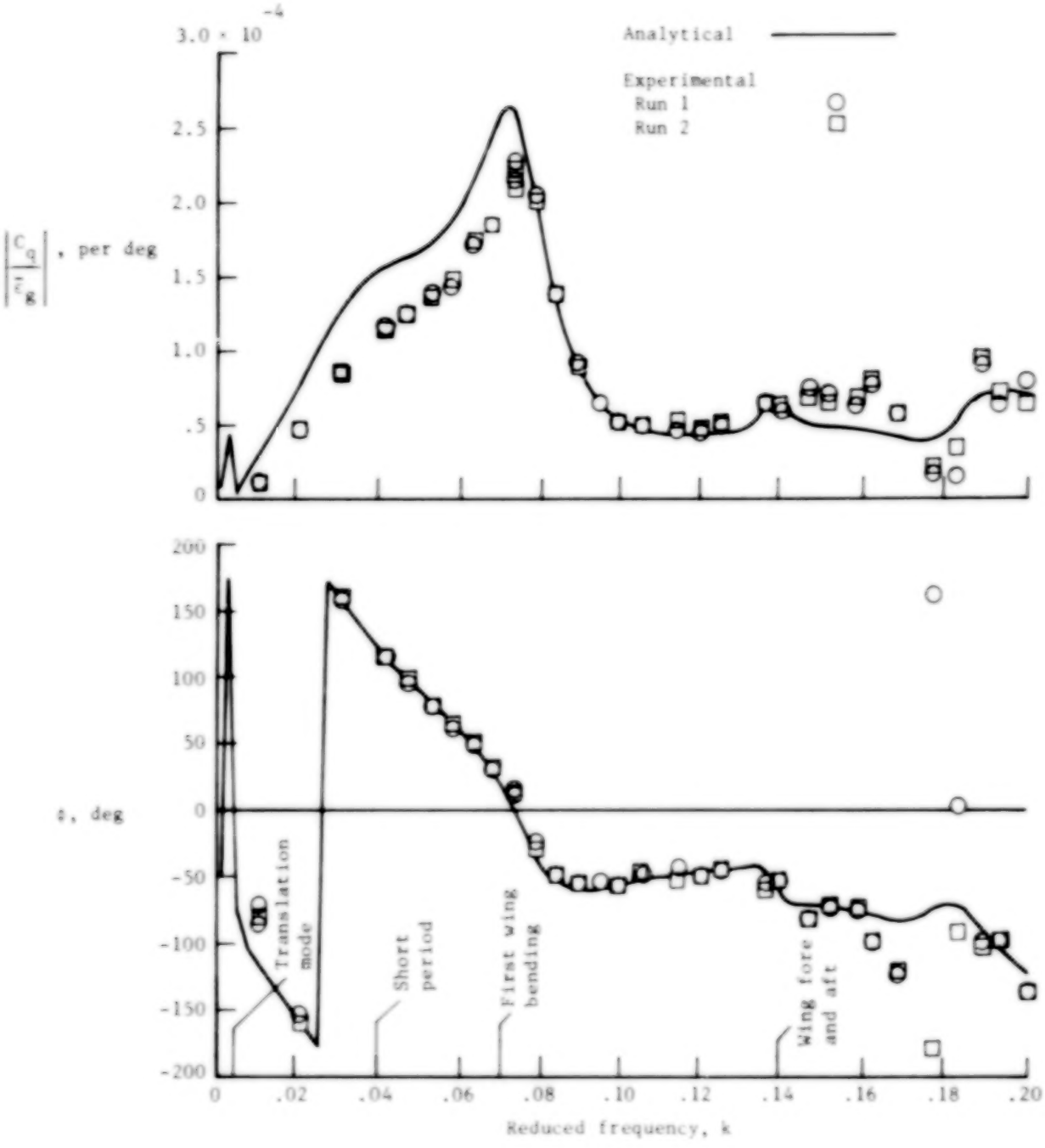

(d) Pitching moment at fuselage station 68.58.

Figure 14.- Continued.

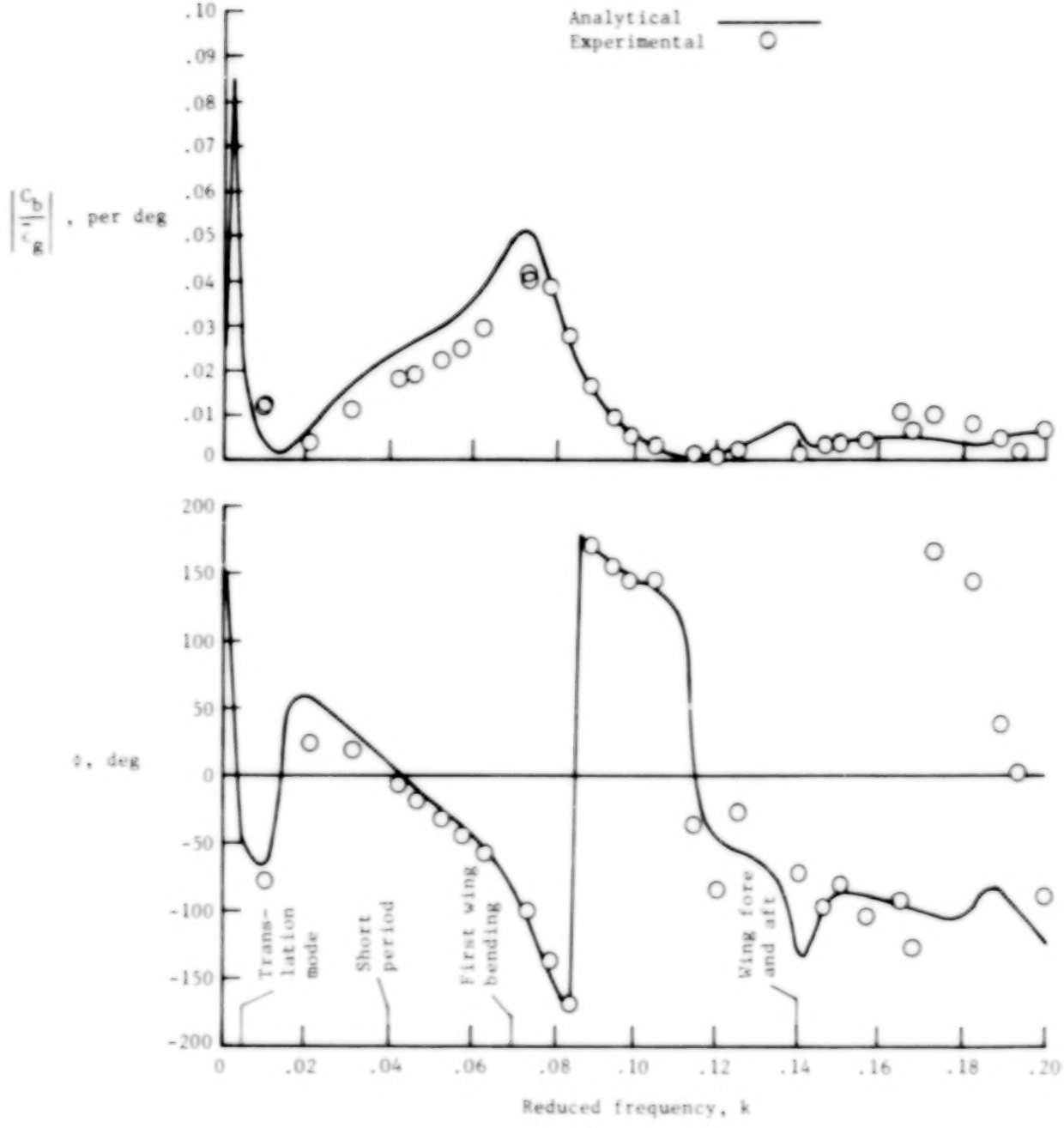

(e) Wing bending moment at wing station 18.80.

Figure 14.- Continued.

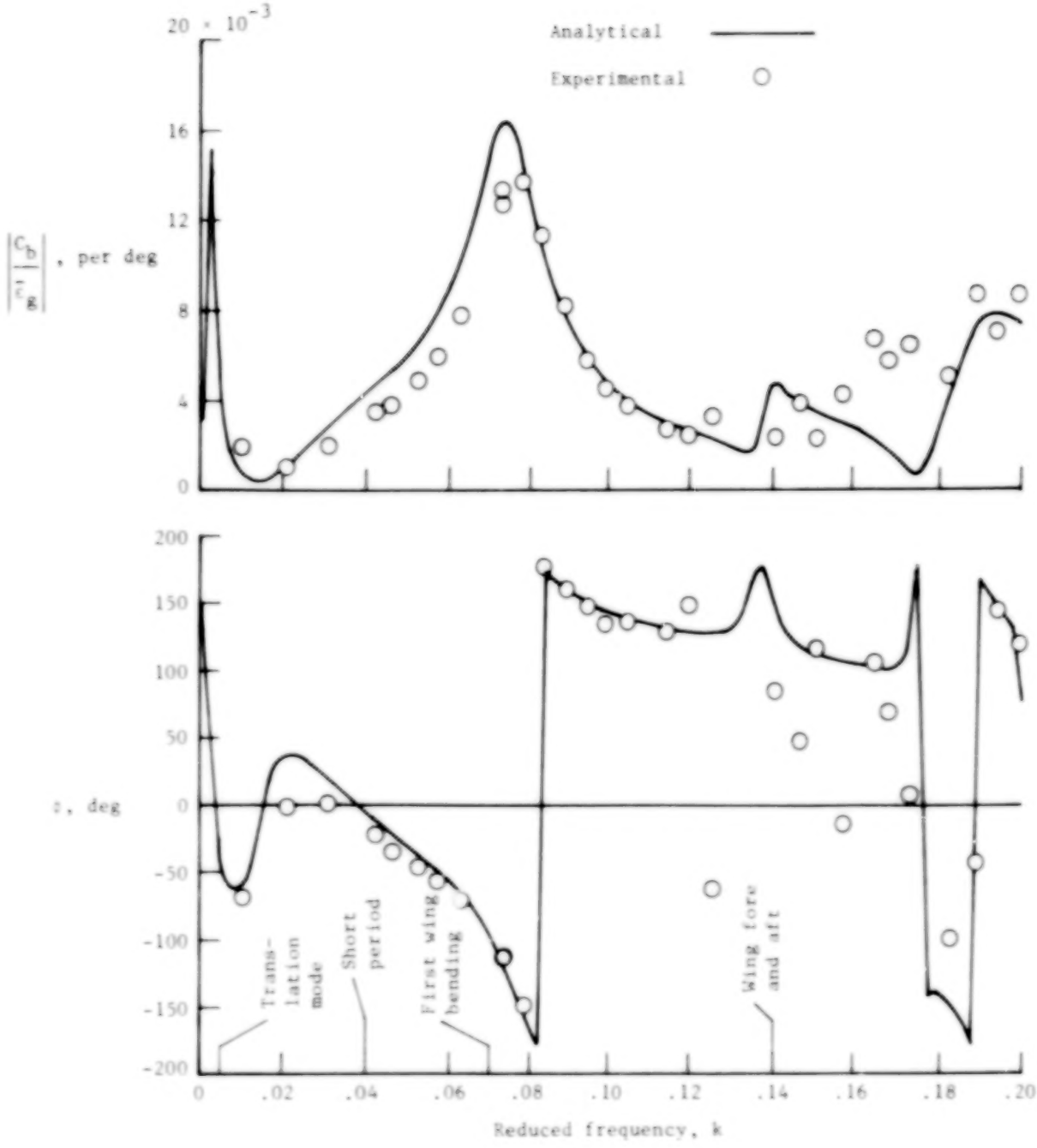

(f) Wing bending moment at wing station 69.43.

Figure 14.- Concluded.

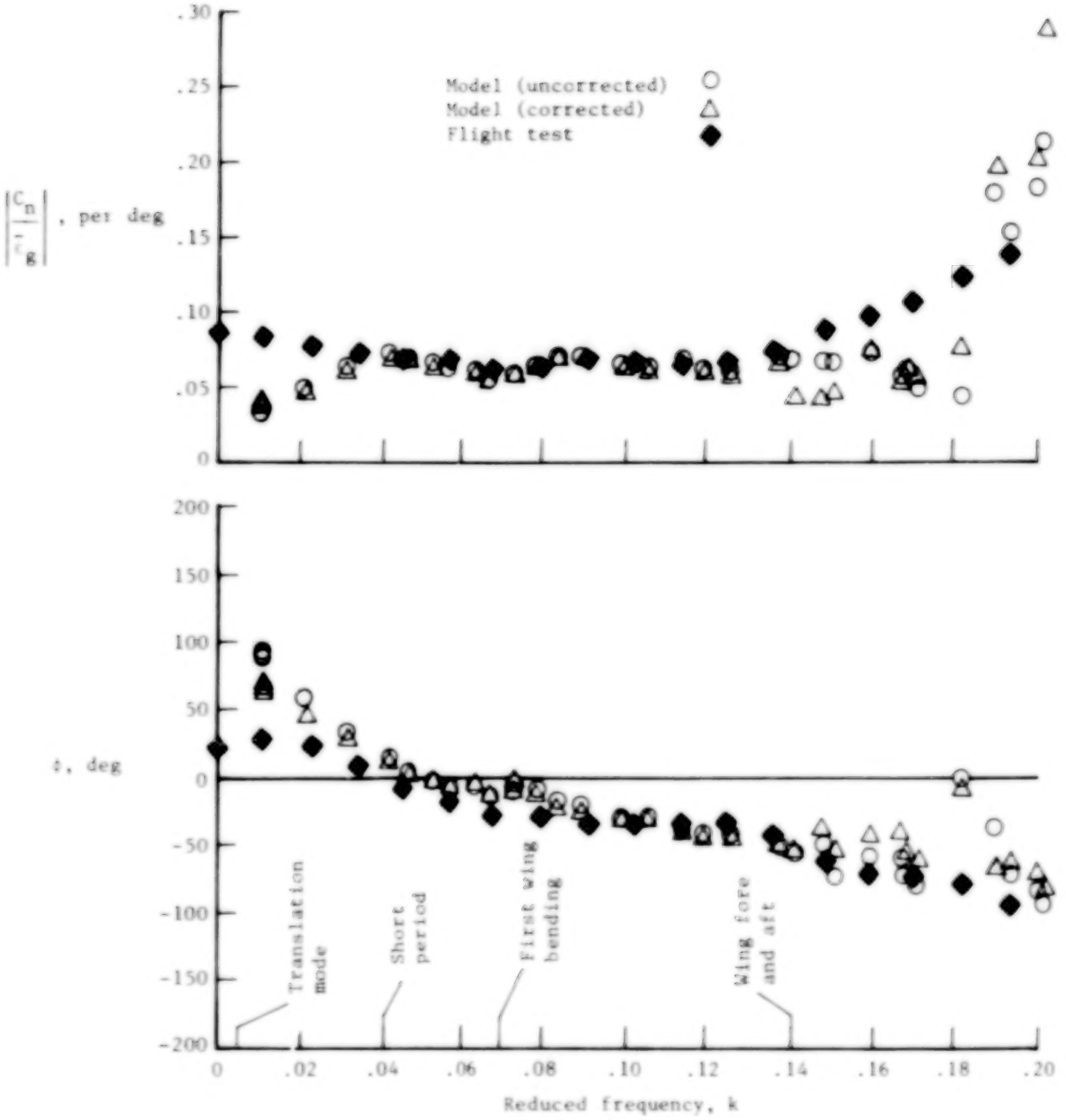

(a) Normal acceleration at fuselage station 9.65.

Figure 15.- Comparison of measured model and airplane frequency-response characteristics.

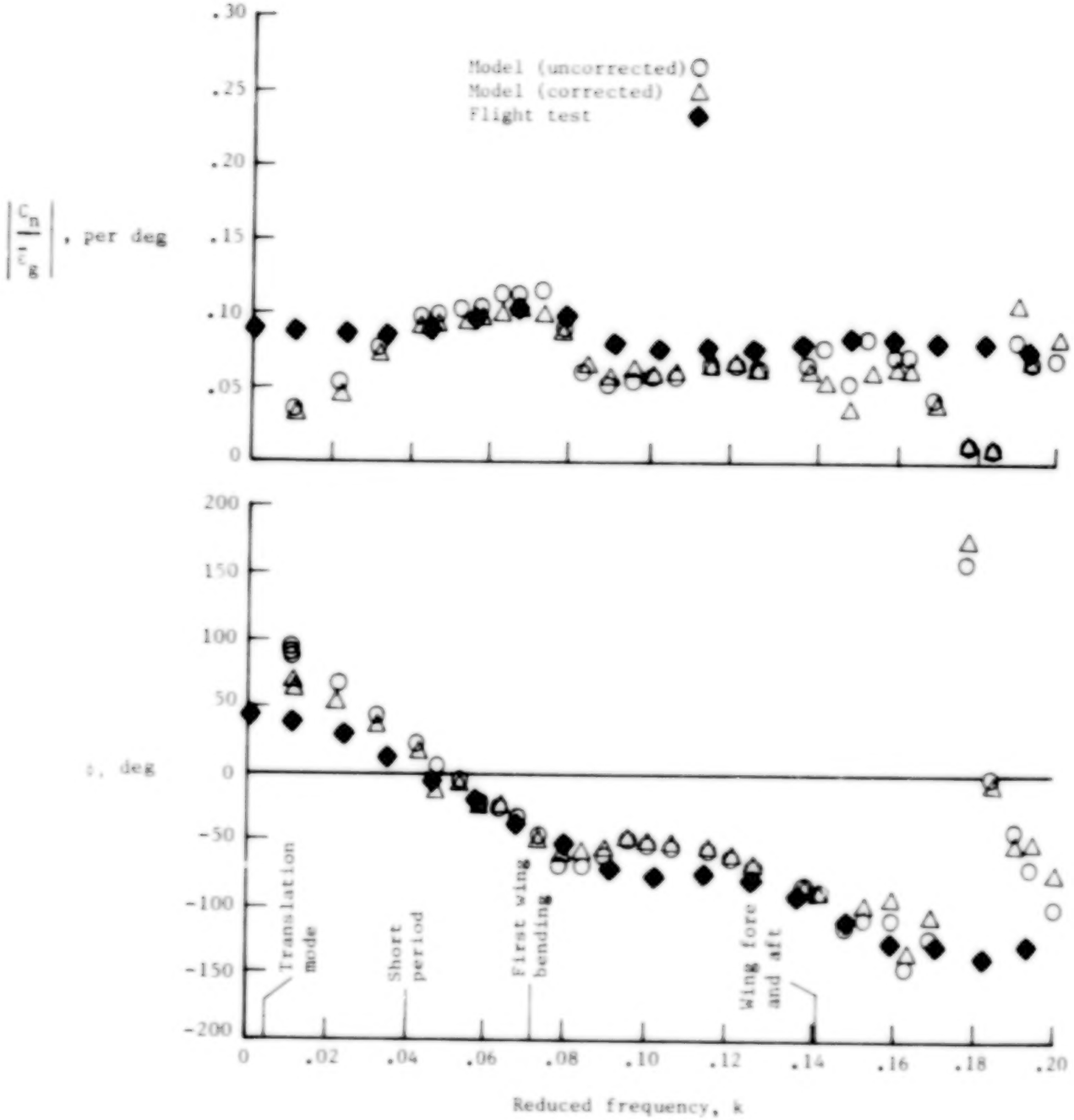

(b) Normal acceleration at fuselage station 68.58.

Figure 15.- Continued.

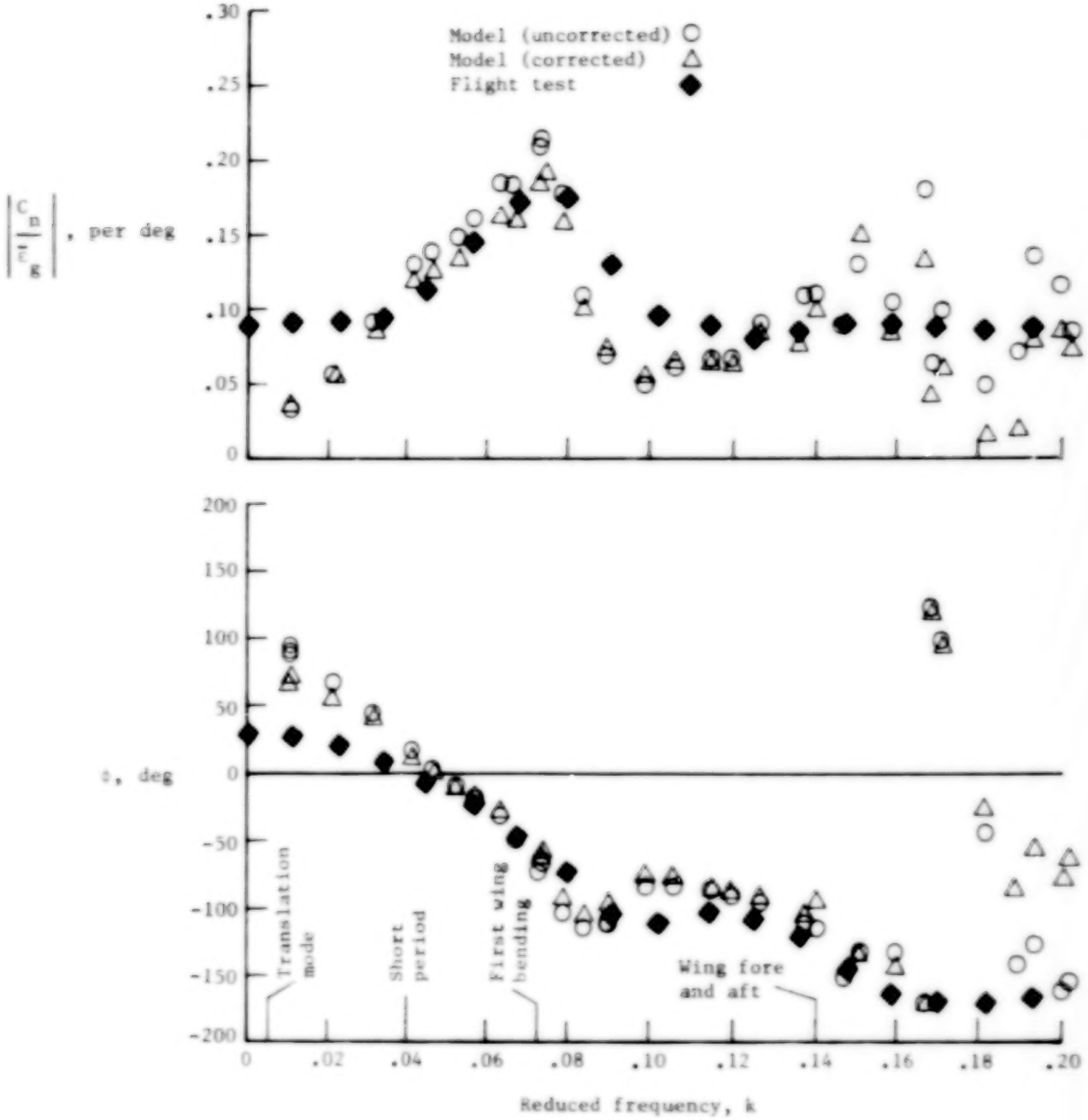

(c) Normal acceleration at fuselage station 135.89.

Figure 15.- Continued.

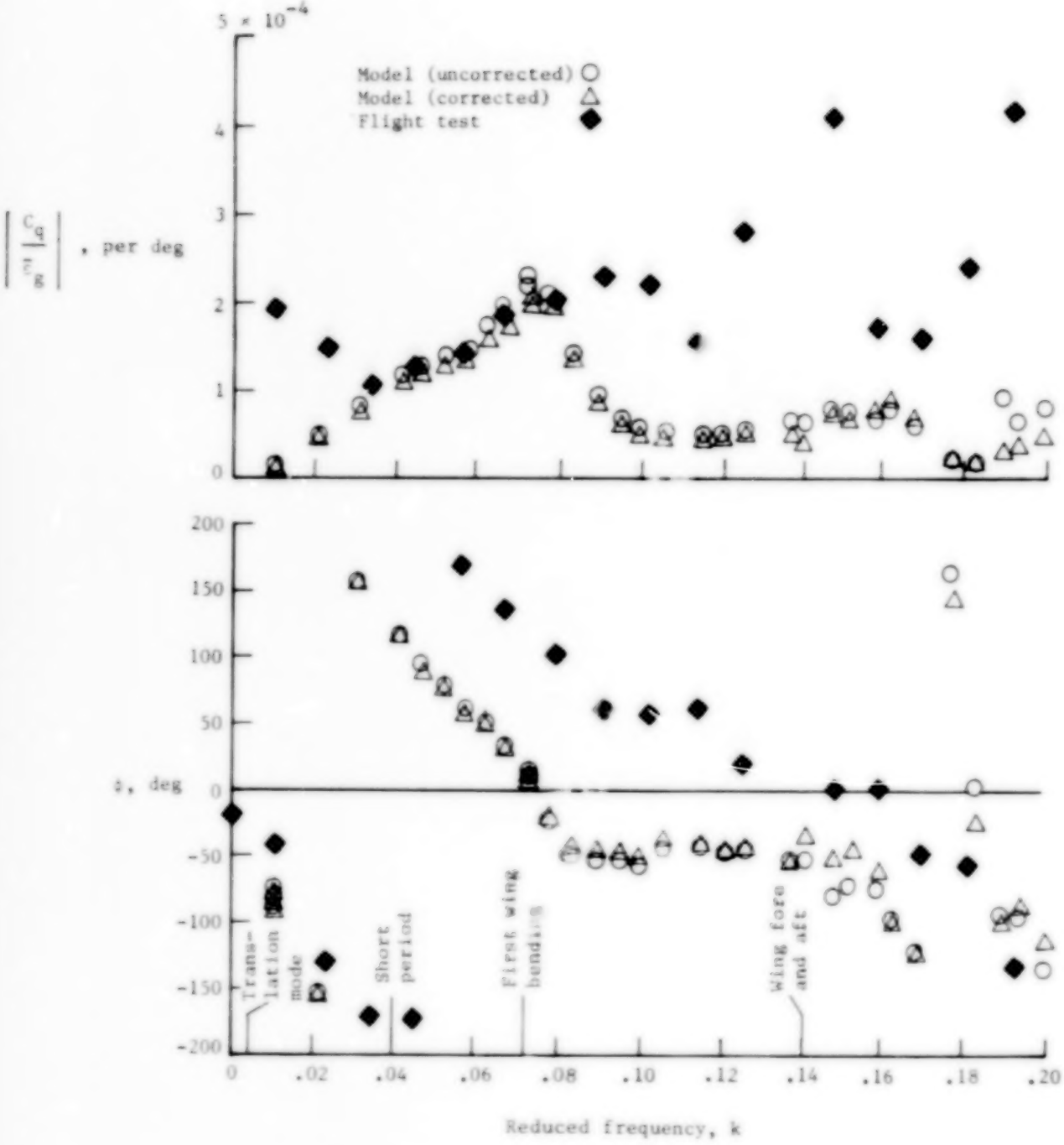

(d) Pitching moment at fuselage station 68.58.

Figure 15.- Continued.

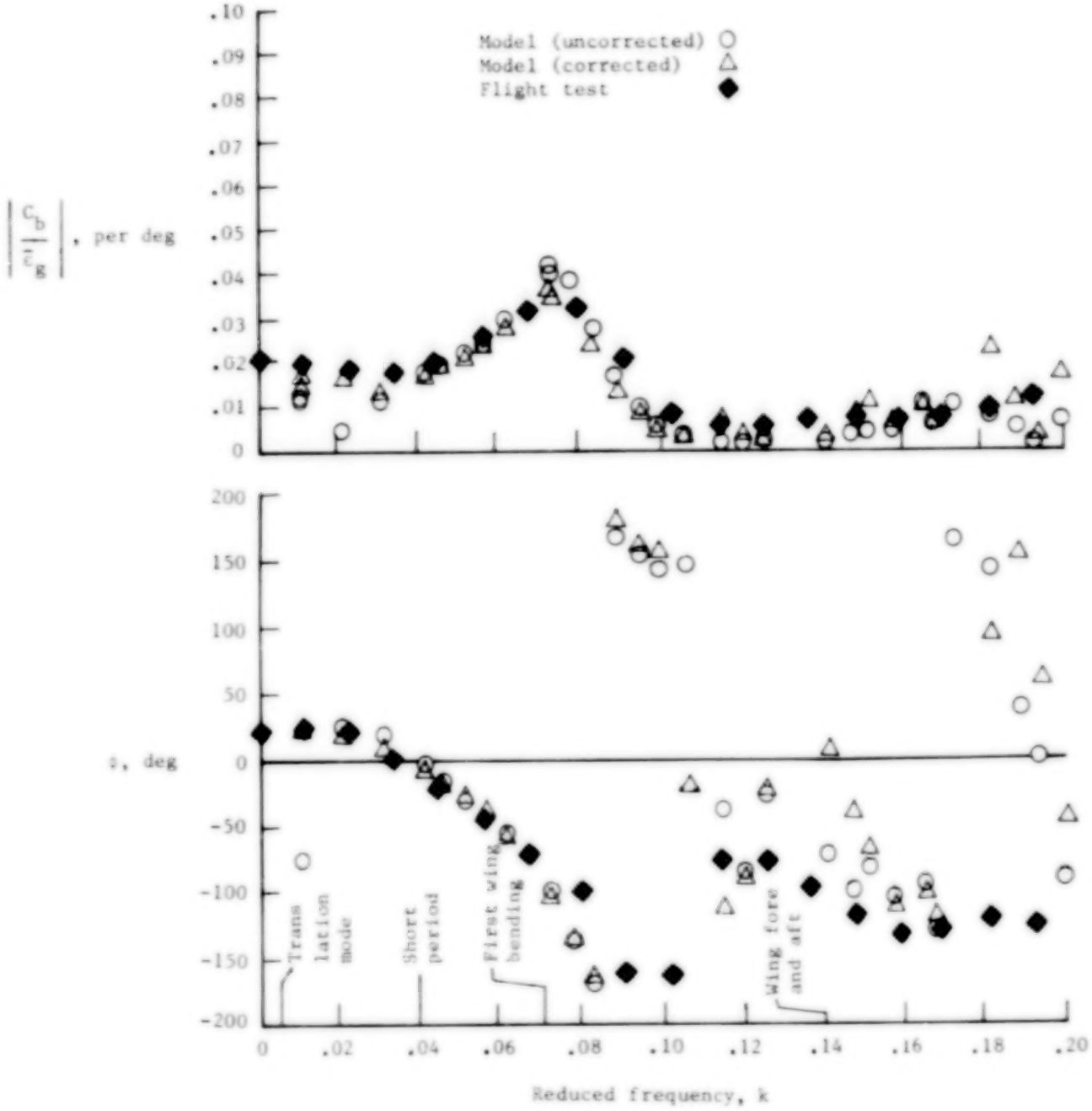

(e) Wing bending moment at wing station 18.80.

Figure 15.- Continued.

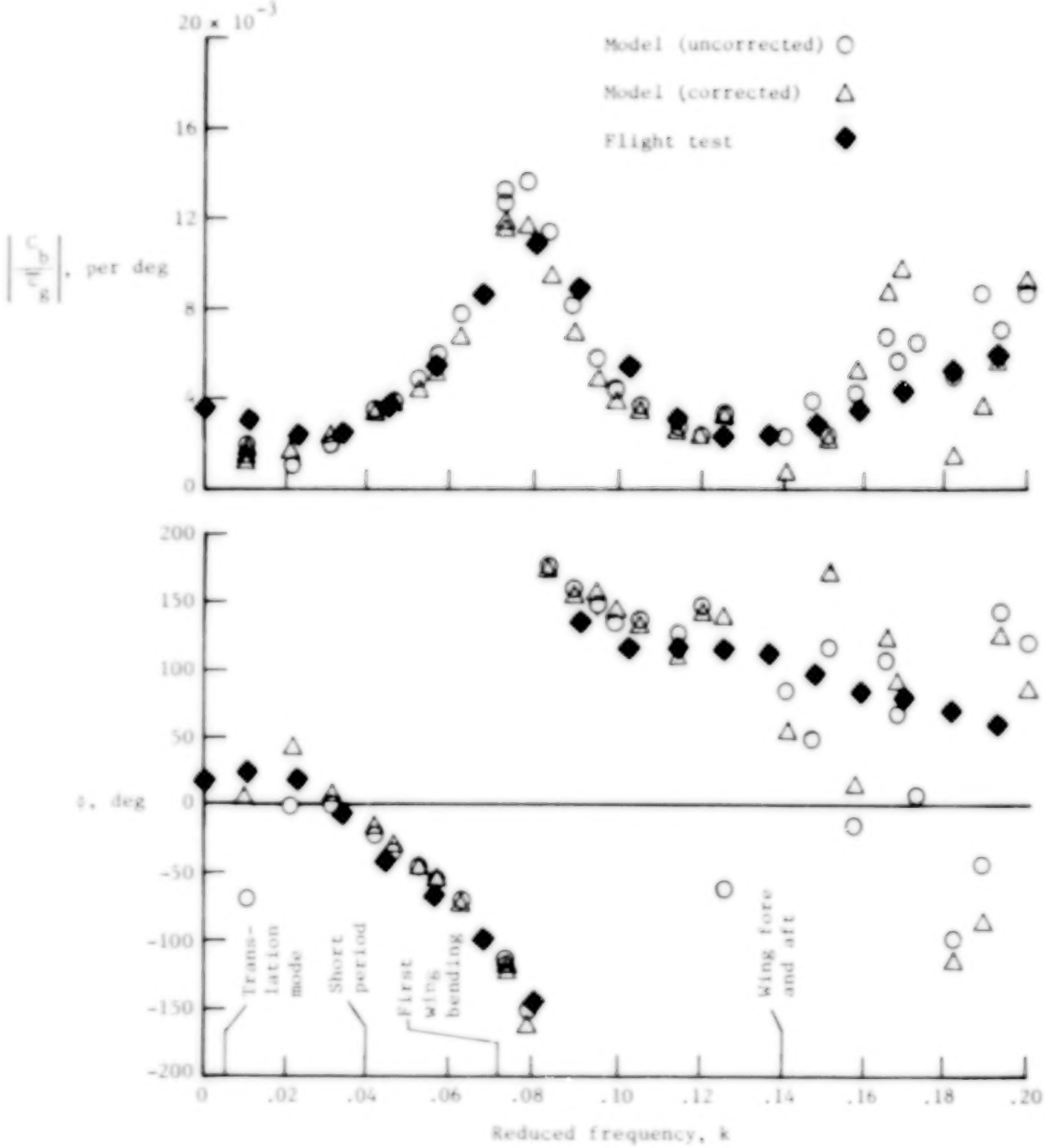

(f) Wing bending at wing station 69.43.

Figure 15.- Concluded.

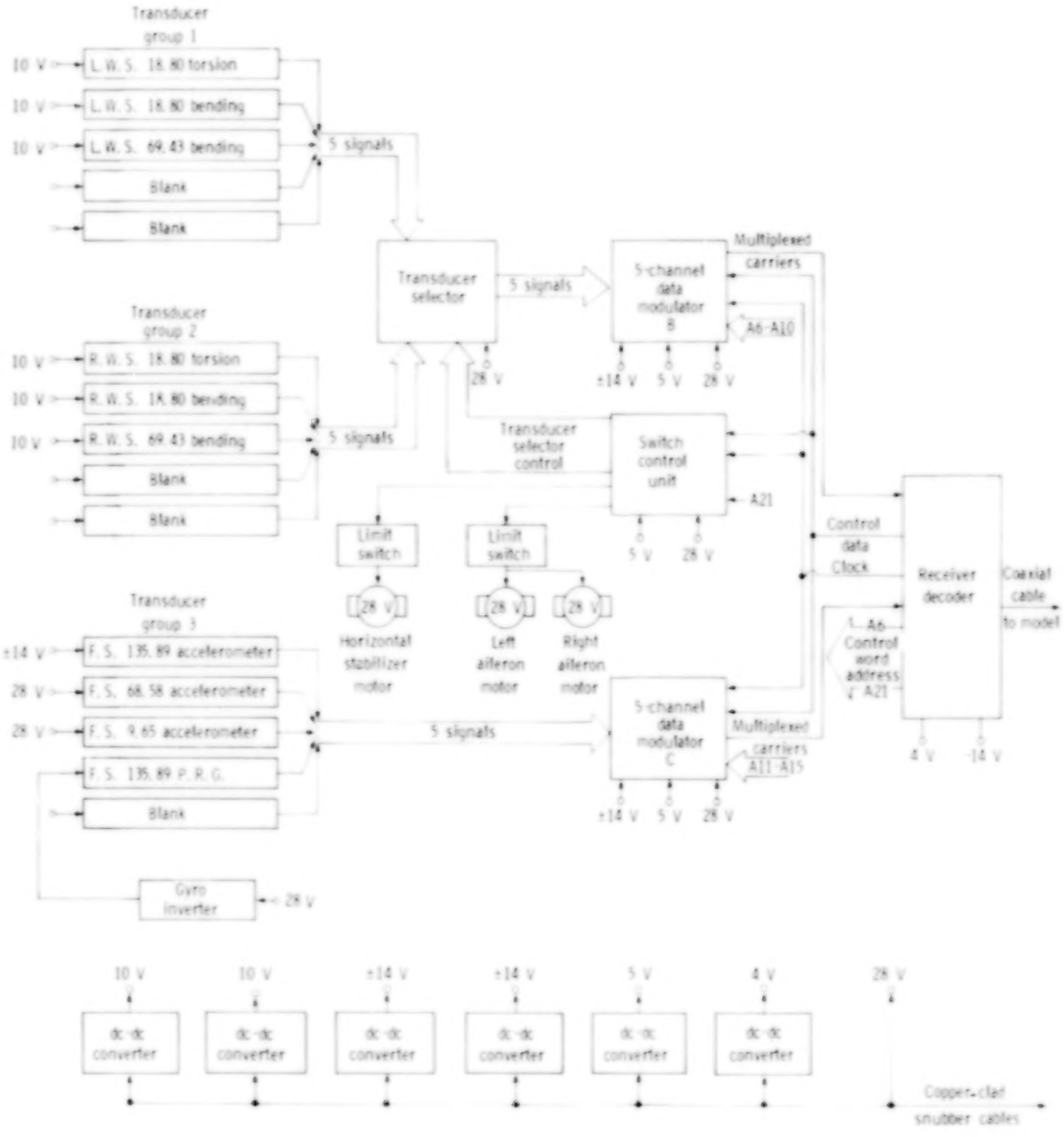

Figure 16.- Block diagram of microelectronic data system.

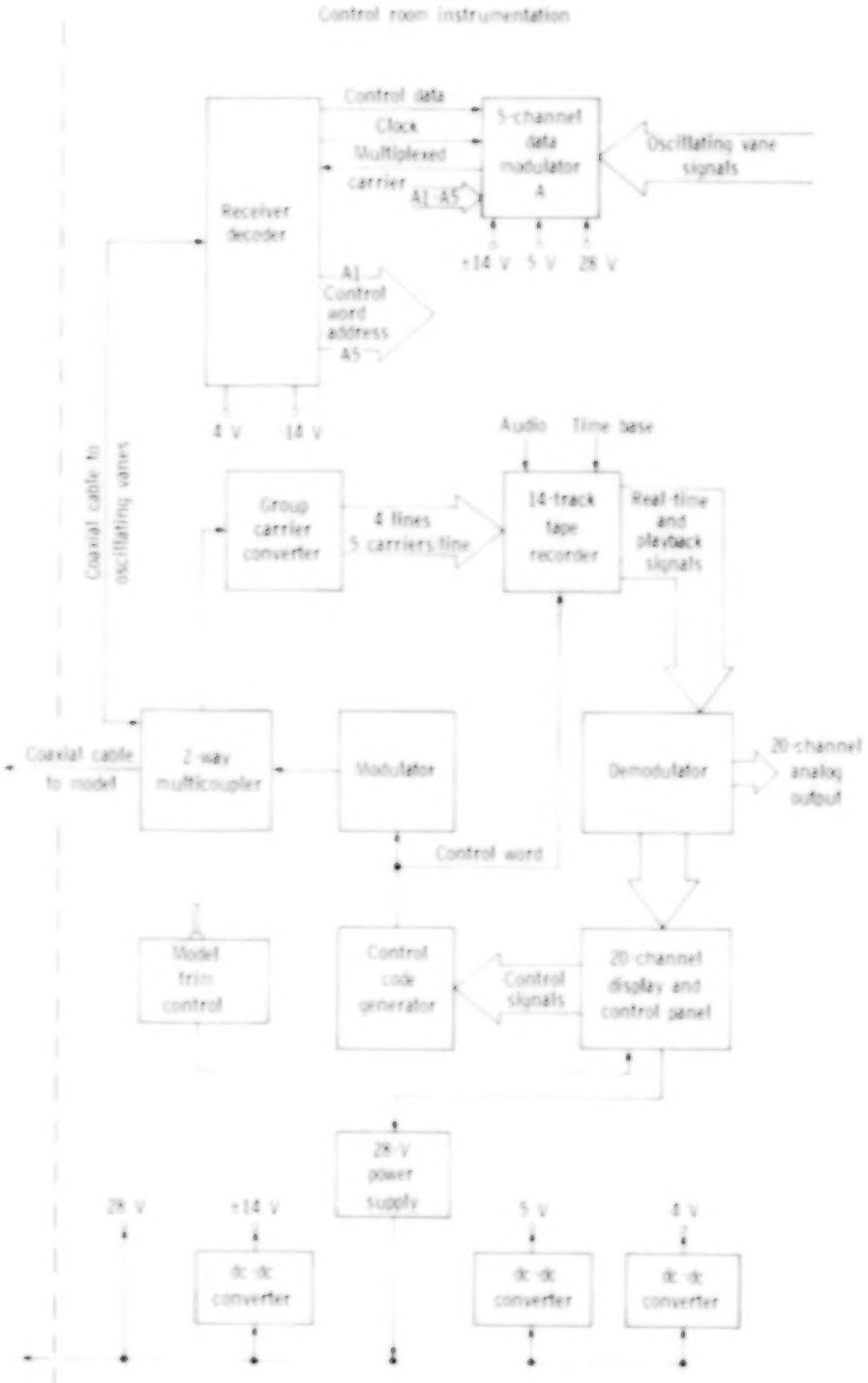

Figure 16.- Concluded.

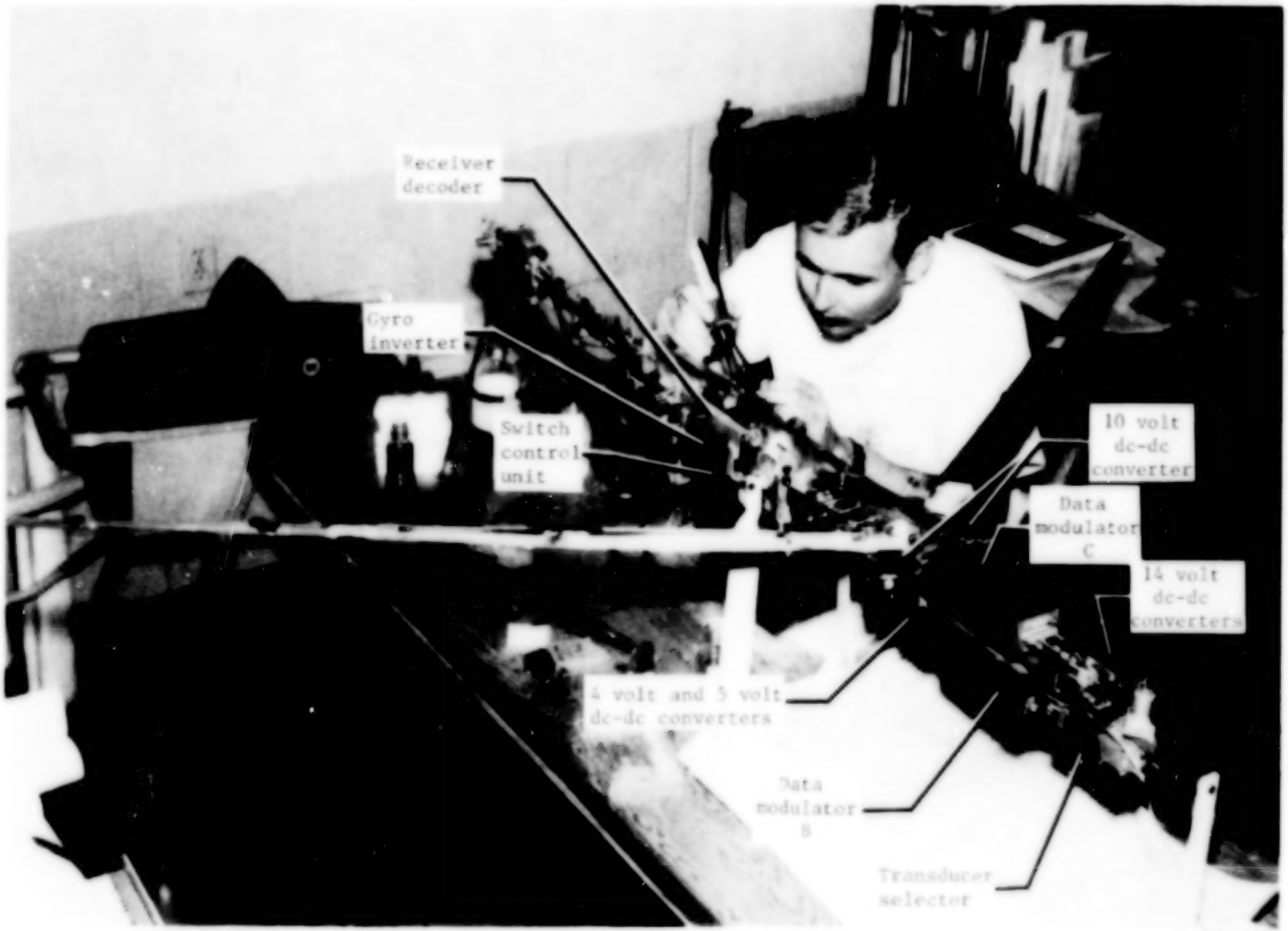

L-79-311

Figure 17.- Arrangement of microelectronic data system components in model.

1 Report No.	2 Government Accession No.	3 Recipient's Catalog No.
NASA TP-1501		

4 Title and Subtitle	5 Report Date
EVALUATION OF A WIND-TUNNEL GUST RESPONSE TECHNIQUE INCLUDING CORRELATIONS WITH ANALYTICAL AND FLIGHT TEST RESULTS	November 1979
	6 Performing Organization Code
7 Author(s)	8 Performing Organization Report No.
L. Tracy Redd, Perry W. Hanson, and Eleanor C. Wynne	L-13137
	10 Work Unit No.
9 Performing Organization Name and Address	505-33-53-01
NASA Langley Research Center Hampton, VA 23665	11 Contract or Grant No.
	13 Type of Report and Period Covered
12 Sponsoring Agency Name and Address	Technical Paper
National Aeronautics and Space Administration Washington, DC 20546	14 Sponsoring Agency Code

15 Supplementary Notes

16 Abstract

A wind-tunnel technique for obtaining gust frequency-response functions for use in predicting the response of flexible aircraft to atmospheric turbulence is evaluated by comparing the tunnel test results for a dynamically scaled cable-supported aeroelastic model with analytical and flight data. The wind-tunnel technique, which employs oscillating vanes in the tunnel throat section to generate a sinusoidally varying flow field around the model, was evaluated by use of a 1/30-scale model of the B-52E airplane, for which considerable flight gust response data were available. The studies show good correlation between the wind-tunnel results, flight test results, and analytical predictions for response in the short-period and wing first elastic modes of motion, which are the modes of primary significance for response of flexible aircraft to atmospheric turbulence.

17 Key Words (Suggested by Author(s))	18 Distribution Statement
Gust Frequency response Wind-tunnel technique Atmospheric turbulence Aeroelastic mode	Unclassified - Unlimited Subject Category 01

19 Security Classif. (of this report)	20 Security Classif. (of this page)	21 No. of Pages	22 Price*
Unclassified	Unclassified	52	$5.25

*For sale by the National Technical Information Service, Springfield, Virginia 22161

NASA-Langley, 1979